Ageing Assessment of Power Transformer Kraft Paper Insulation Using Optical Speckle

By

Hamid Hassanzadeh Khakmardani

A thesis submitted to the Faculty of Graduate Studies of

The University of Manitoba

In partial fulfillment of the requirements for the degree of

MASTER OF SCIENCE

Department of Electrical and Computer Engineering

University of Manitoba

Winnipeg, Manitoba, Canada

Abstract

Power transformers play an important role in electric networks. Copper windings wrapped in kraft paper and immersed in a tank of mineral oil are their main composition. Oil-impregnated paper is a very common insulator in power transforms, due to its durability and endurance. Kraft paper, a wood-based fiber from cellulose, can gradually degrade due to the ambient effects such as high-voltage electric field, temperature, and moisture in the normal working condition of transformers. Aged paper is more prone to experience electric breakdown which finally results in transformer failures. It is essential to monitor paper insulation condition. Conventional methods for evaluating kraft paper are mainly based on chemical analyses which require sampling of the surrounding oil and are usually time-consuming and expensive.

Investigation on and classification of aged kraft paper with four different levels of thermal ageing using a potentially fast, simple, and inexpensive optical setup based on optical speckle is the main subject of this thesis. Speckle interference patterns from a laser diode source have been captured by a CCD camera. Classification based on textural features shows very good discrimination between ageing classes making this technique promising for industrial applications.

Acknowledgements

I am very thankful to my advisors, Drs. B. Kordi and S. Sherif who supported me with very positive and helpful comments and guidance. They really enhanced my enthusiasm toward the topic. I am also grateful to those who constantly supported me with their valuable feedbacks, conversations, and lab equipment. Also I would like to extend my gratitude to the examining committee, Drs. D. Swatek and P. Irani for their time to review this thesis and their constructive comments.

I would like to acknowledge the financial support from the Faculty of Graduate Studies of the University of Manitoba, Manitoba Graduate Students funds, and Natural Sciences and Engineering Research Council of Canada (NSERC). I am also thankful to all my colleagues especially Nathan Jacob for providing paper samples and close collaboration. I would like to thank the staff of the Department of Electrical and Computer Engineering including Amy Dario for administrative helps and Cory Smit for accurate cuts of optical bread-board. And last but not least, my special thanks go to my wife and also the family back home for all their support, encouragement, and patience.

Dedicated to

My beloved grandfather, Agha Esmaiel, who passed away peacefully...

12 Aban 1393 – Nov.3, 2014

Table of Contents

List of Tables

List of Figures

Chapter 1

Introduction

1.1 Background

Importance of power transformers as one of the major components between generation and distribution stations is the foremost among other contributing elements in power transmission networks; they have the huge task of transferring electric power within the power network. A typical power transformer has the combination of both liquid and solid insulating material among its conductor windings for proper operation. In the early 20th century, the combination of cellulose and mineral oil was recognized as the standard insulation combination for power transformers [1]. Windings of power transformer are wrapped with kraft paper, while the whole structure is immersed in a tank of mineral oil. Among all different factors that may affect the lifetime of a power transformer, insulation material is known to be very critical [1]. Liquid insulation, *i.e.* mineral oil, in a power transformer is readily accessible and also reusable after proper refinery processes, but solid insulation *i.e.*, kraft paper is the permanent component of the insulation system which is less accessible for condition assessment [1].

Due to presence of numerous power transformers in the province of Manitoba/Canada as an exporter of the electric energy to other provinces[1], assessment of the condition of operating transformers and also preventing unforeseen failures are of great importance for planning and on-time maintenance purposes [2]. This provides high motivation to investigate and develop new, state-of-the-art techniques for better on-line and/or *in-situ* condition assessment of aged power transformers via potentially non-invasive, fast, direct and accurate optical methods. Investigation and classification of kraft paper samples with different levels of thermal ageing by means of a potentially fast, simple, and inexpensive optical setup based on laser speckle phenomenon is the main subject of this thesis. Driven by an industry-induced motivation, laser speckle phenomenon has been investigated in this thesis to provide a potentially simple and fast setup for condition assessment of the kraft paper in oil-immersed power transformers.

1.2 Problem Definition and Existing Solution

The problem with kraft paper is that it loses its electrical and mechanical strength due to ageing. Aged paper is more prone to experience electric breakdown which finally results in transformer failure. Kraft paper is basically a wood-based material mainly composed of

---

[1] In the fiscal year of 2012-2013, from the total of electricity export sales of Manitoba Hydro ($353 million), 88% was sold in the U.S. market and 12% in Canadian markets [2]. Also according to the latest Manitoba Hydro Electric Board 62nd Annual Report, with the 5,685 megawatts of installed electricity generating capability, almost one-third of the total average electric energy produced annually (32 billion kilowatt hours) has been exported in 2012-2013 (9.1 billion kilowatt hours).

cellulose, as the most frequent organic polymer on Earth [3]. Ageing in the paper insulation has been identified by chemical and physical changes. Conventional methods for evaluating kraft paper are mainly based on chemical approaches. Reaction of paper and oil in presence of oxygen and moisture (water content) with electric and thermal stresses changes the percentage of chemicals especially gases in the transformer tank. The chemical methods are usually time-consuming, expensive, usually offline, and indirect that require sampling of the transformer paper. Sampling of the transformer oil, on the other hand, could be done online however due to circulation of the oil, it cannot identify the location of the defects [4].

On the other hand, various optical methods have been used for the investigation of paper properties and quality assurance purposes in paper and pulp industry for a while. Most of them such as scanning electronic microscopy (SEM), regular imaging, optical coherence tomography, profilometry, and gloss meters are direct approaches which give information about the physical structure of the paper [5], [6], [7]. The optical methods, usually are complex and expensive which have less potential to be used as online condition assessment diagnostics for operational power transformers. Also there have been less attention to the application of laser speckle for insulation assessment of power transformers. The aforementioned issues motivates performing this research and feasibility study for using laser speckle in power transformer applications.

1.3 Objective of the Thesis

Prevention of unforeseen transformer outages will increase system reliability and customer satisfaction. Also from management point of view, better planning of time and budget resources required for system maintenance and utility upgrades, will be enhanced by more accurate asset management approaches given by projects of this type [8]. From a general view, risk/benefit analysis based on online, regularly-updated condition assessment reports, is an asset for power industries. In this regard, the methodology presented in this project is summarized as the follows.

In this research, we are investigating the physical changes of paper insulation due to accelerated ageing and the effect of ageing time and temperature. Classification of paper samples based on different ageing levels will provide the potential to estimate life-expectancy of the power transformer and scheduling timely maintenance before disastrous transformer failures happen.

Focus of this project is to develop techniques to discriminate different ageing levels of oil-immersed power transformer paper insulation by means of an optical phenomenon related to the nature of laser light, named laser speckle. "Optical speckle" is the widely used phrase to describe the optical phenomenon associated with grainy intensity patterns due to self-interference of light [9]. The optical methods can be considered as direct investigation methods with potential of non-invasive measurement and implementation; but they are still

not mature enough to be used as routine online condition assessment tools for power transformers. The industrial applications of laser speckle as an optical phenomenon are diverse. However, not a significant number of publications are available for the special application of using speckle phenomenon to identify ageing of paper insulation in the power transformers [10].

The aim of this thesis is to study the feasibility of using laser speckle phenomenon to classify ageing levels of kraft paper as the basic solid insulation material in power transformers. This thesis is a part of a larger project to study the potential of using optical methods such as imaging, microscopy, interferometry, and spectroscopy based on fiber optics or other convenient implementation substrates to be integrated with currently operational transformers. Such proposed technologies can also be implemented as portable diagnosis instruments for field measurements of paper insulation condition in power transformers. The future goal is to develop an online *in-situ* system enhanced with capabilities of automated machine learning algorithms to identify ageing level of power transformers.

1.4 Thesis Contributions

- By using laser speckle phenomenon as an optical method, physical changes in the paper insulation due to thermal ageing is distinguishable. These physical changes can be correlated to the ageing level(s) of the paper in a power transformer. Therefore, the proposed optical imaging method in conjunction with automated

computer classification on textural features [11] of the acquired paper images can be used to differentiate paper samples. This differentiation of insulating paper is a useful diagnosis tool with added values for transformer maintenance procedures due to the accuracy and simplicity of the setup.

- In this project a simple laser based illuminating source has been implemented on a microscope which gives the ability of capturing speckle interference patterns via the CCD camera installed on the bottom port of the microscope. Speckle patterns of paper samples produced by the laser diode source has been captured with a CCD camera in two imaging modes of transmission and reflection. The potentially inexpensive and simple setup with the laser diode source confirms the potential of this technique for industrial application[1]. [12]

- Using the extracted textural features of the acquired speckle interference patterns, a very good classification of aged papers with well-known linear and non-linear pattern recognition classifiers has been achieved.

1.5 Thesis Outline

The thesis is arranged in 6 chapters as follows. Chapter 2 is on insulation material and its importance for determining life expectancy of the power transformers. Traditional

---

[1] Also in contrast to the other metrological measurements of the paper, there is no need for successive speckle photography which usually requires change of wavelength or incident angle of light as regularly done for roughness measurementas mentioned in p.123, chapter 9 of [12].

assessment methods such as "dissolved gas analysis", (DGA) and "degree of polymerization", (DP) measurements have been reviewed and their limitations are discussed. Chapter 3 is a brief review of the origin of the optical speckle phenomenon as an interferometry pattern produced by the nature. This chapter also covers the application of the speckle phenomenon and related work for characterizing paper. Chapter 4 describes the methodology of experiments including sample preparation and optical setup. Both transmission and reflection mode imaging schemes for speckle capturing have been presented with practical details. Chapter 5 presents the results and analysis which include the steps of a typical classification problem as data collection, feature extraction, feature selection, classifier, and performance evaluation. Chapter 6, finally, includes conclusions and future work.

Chapter 2

Paper Insulation in Power Transformers

In this chapter a brief review of power transformers and their common problems with special attention to the insulation material are presented. The role of kraft paper, as the most common cellulosic insulation material in oil-immersed power transformers, will also be presented. Thermal ageing as the dominant cause of paper degradation is also discussed.

2.1 Power Transformers

In AC[1] systems, transformers are static electrical devices that operate based on electromagnetic induction and have no continuously moving parts. The history of the first operational power transformer goes back to around 130 years ago in the United States. According to the "IEEE Standard Terminology for Power and Distribution Transformers" [13][2] a power transformer is exactly defined as: "A transformer that transfers electric energy in any part of the circuit between the generator and the distribution primary circuits." In general, based on the complexity of the electric power network, at each point of voltage level transition, a power transformer is required [1]. Power transformers can be used to step-

---

[1] Alternating Current
[2] Clause 3.327 page 28 of IEEE Standard C57.12.80-2010.

up from generation voltage to the transmission voltage or to step-down from transmission voltage to the distribution voltage.

2.2 Core and Winding in a Power Transformer

A core and winding, surrounded with the insulating material, construct the main structure of a power transformer. Core of the transformer provides the main path for the magnetic flux. Core usually consists of thin laminated stripes of steel with thickness in the range of 0.23 mm to 0.36 mm, packed together and insulated electrically from surrounding structures. It can be constructed in two different general topologies named: "core-type" or "shell-type" with either circular or rectangular cross-sections (see Figure 2.1) [1].
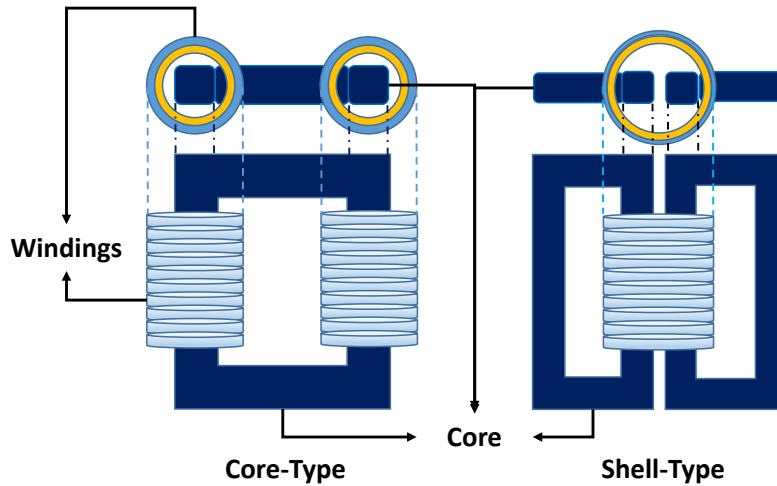
Figure 2.1 Core-type and shell-type for a single phase transformer winding with rectangular cross section for the core. In core-type construction, only one path for magnetic flux exists.

Windings, or interchangeably transformer coils, are insulated conductors wound around the core. For the winding material, aluminium with the benefits of light-weight and lower cost is competing with copper which has higher current carrying ability. Coil lead is the conductor connection between a winding to the final termination point which could be a terminal, bushing or another winding[1]. Coil cross overs are positions of the conductor which it is deflecting in parallel toward a neighboring adjacent position to construct a new turn or termination end. Schematic of coil lead and cross overs has been depicted in Figure 2.2.
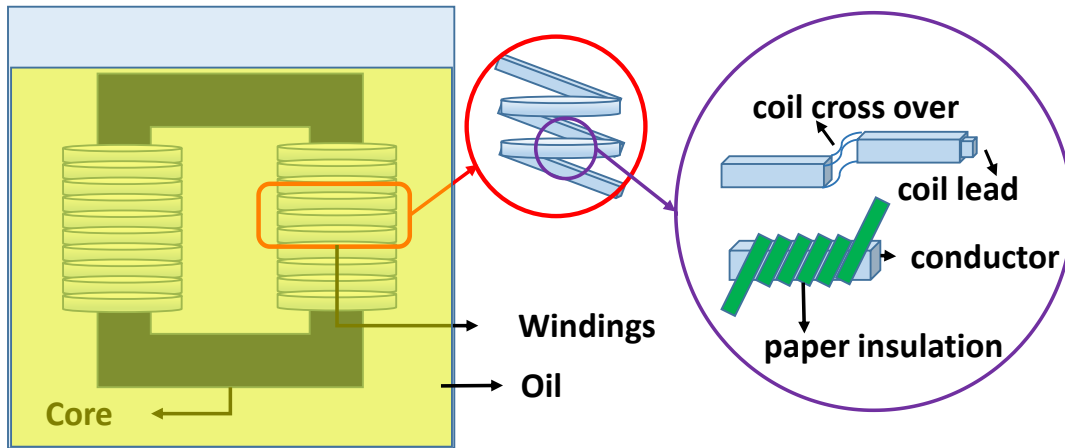
Figure 2.2 Simplified schematic of the paper insulation wrapping around the conductor winding of an oil-immersed power transformer.

In the insulation system of a typical power transformer there exist hot spots for the insulation paper in which paper undergoes more mechanical tension or non-uniformity in wrapping such as coil cross overs and coil leads. To have a better understanding of the

---

[1] Based on the definition in part 3.222 of IEEE C57.12.80-2010 Standard Terminology for Power and Distribution Transformers [13].

insulation system, it is worth pointing out these locations, especially for sampling purposes (if possible). Insulation system in a power transformer should include insulation of each individual winding, insulation of low voltage (LV) and high voltage (HV) sections and turns from one another, plus insulation of windings to the tank and grounded core as it will be mentioned in Section 2.9.4.

Power transformers can be classified based on the insulation level, cooling class, and power ratings. For the insulation, cellulosed based paper and mineral oil is the most frequently used combination in the oil-immersed power transformers with copper or aluminum windings[1]. The winding and the core of transformers are known as the main sources of heat generation due to magnetic core loss and ohmic conductor loss. Usually, indoor transformers are dry-type. On the other hand outdoor transformers are usually liquid-immersed.[14]

Natural convection helps heat transfer from the core and windings to the tank and surrounding environment via "thermosiphon" effect. Cooling class of the power transformer depends on the application, load condition, and heat transfer schemes. It can vary from simple air-cooled transformers to forced circulation transformers, enhanced with oil pump, radiator, fans and external air/water heat exchangers. In general, transformers with higher

---

[1] Research is ongoing to use nano-materials as insulator and superconductors as conductor in the next generation of transformers [14].

cooling class have higher ratings. Figure 2.3 shows a typical three phase oil-immersed power

transformer which cooling radiators are visible in the photograph.

Figure 2.3. A typical 3 phase power transformer under test at the High Voltage Test Facility (HVTF) of Manitoba Hydro (Photo by author, July 2014).

2.3 Insulation Material in Power Transformers

As stated earlier, a typical outdoor power transformer employs a combination of liquid[1] and

solid insulating material for proper operation. In the beginning of 20th century, the

combination of cellulose and mineral oil was recognized as the standard insulation material

combination for power transformers [1].Windings of the power transformer are wrapped

---

[1] Other alternating insulating liquids such as Natural Ester and Envirotemp™ FR3™ fluid with the benefits of being environment friendly(green) have been proposed to replace with commonly used mineral oil [52], [53] but for very cold temperatures (~ -40ºC in winter time in Manitoba), mineral oil is still commonly used.

with kraft paper, while the whole structure is immersed in oil. Kraft paper, as the solid insulation material, isolates the windings electrically[1]. On the other hand mineral oil as the liquid insulation material has two major roles: (a) It enhances the dielectric properties of the paper by filling the air voids in cellulose fibers of the paper, and (b) acts as a circulating coolant for heat transfer among internal structure of the power transformer. Depending on the situation, solid insulating material in a typical power transformer has the role of mechanical support (pressboard) and thermal insulation in addition to electrical insulation[1].

2.4 Importance of Insulation

Power transformers are designed to be operational for a number of decades. It is important to consider that the life time of the solid insulation material basically determines lifetime of the power transformer. Since there is no moving part in the transformer tank, no wear and tear occurs, but stress factors such as thermal and electrical stress can age, degrade, and eventually deteriorate the insulating material which reduces the typical life expectancy of the power transformer [1].

Considering insulation, combination of liquid and solid insulation has been well established for power transformers. Mineral oil can be drained and replaced based on the level of oil

---

[1] It is also worth mentioning that "pressboards", composed of thick layers of compressed cellulose are also used to sectionize windings and provide a mechanical support and separator for each winding section.

degradation, but solid insulation (paper among windings) cannot be replaced without de-tanking the transformer.

To have an estimate of the amount of insulation in a typical power transformer, reference [4] gives an example of a 600 MVA transformer which contains 12 tons of paper (with 30-120 µm thickness of each layer) and 40,000 liters of oil.

2.5 Kraft Paper – Terminology and Background

The German word "Kraft" means "strong". In the realm of paper and pulp industry, "kraft paper" refers to "strong paper or cardboard from wood pulp". Kraft paper in general is a brownish, unbleached paper used for packaging purposes. It can also refer to a class of electrical insulation paper [15].

Since early 20th century, cellulose based paper and pressboard have been candidates for oil-immersed transformers. Later on, thermally upgraded paper, widely used by transformer industry in 1960s [16] was introduced. Structural properties of paper, whether related to surface or volume, affects quality of the paper in different applications, for example in photography applications, coated paper with minimum impurities is desired. In printing applications, filler content of the paper and ink absorption properties is addressed. Paper with homogenous, smooth surface, and less gloss is preferred for retaining ink and easy reading. Also in packaging applications, mechanical strength of paper related to internal structure of paper is more desirable [15]. On the other hand, dielectric strength, tensile

strength, and heat transfer ability of paper are more important in insulating application in power transformers. Therefore, it is important to focus on related properties of paper according to the application. Kraft paper, as an insulating material, has applications in making capacitors, cables, and power transformers. Dielectric strength[1], mechanical strength including tensile strength and tearing strength, and thermal performance of the paper is considered as its requirements for insulating applications [17]. In this thesis, the word "paper" simply refers to "kraft-paper in transformer", unless otherwise stated.

2.5.1 Composition of Kraft Paper

Wood as the source of paper is mainly composed of "cellulose (~40-50%)", "lignin (20-30%)", "hemi-cellulose (10-30%)" and polysaccharides. Lignin is the brownish aromatic element of paper. Lignin and hemi-cellulose are considered as unwanted components for the industrial purpose which are removed from wood for preparing the kraft paper during kraft pulping process [18], [19]. After finishing, cellulosic paper contains ~90% cellulose, ~3% lignin, and ~7%hemi-cellulose [4].

---

[1] Dielectric strength is the maximum electric field that an insulator such as paper can withstand before it electrically breaks down. Tensile strength is the maximum tension that a sheet of paper can withstand before breaking mechanically, and tear strength is the average force required for propagation of a cut in a sheet of paper; these mechanical parameters of paper are closely dependent to the fibre network and their direction in the paper [54].

Cellulose is the basic building block of cell walls of green plants and the most frequent organic polymer on Earth with chemical formula $(C_6H_{10}O_5)_n$[1] which is also biodegradable. Approximately 90% of cotton, 50% of wood and 45% of hemp is cellulose [3]. It is basically a polymer of glucose units. Number of glucose units, is an index of mechanical strength of cellulose-based paper. Average number of these connecting glucose units to each cellulose fiber may be greater than 20,000 units for natural cellulose which is reduced during pulping process to about 1,200 units. This average number is called Degree of Polymerization (DP) or in scientific words, DP is the number of monomer units in the polymer [20].

Cellulose loses its mechanical strength due to ageing, especially in a power transformer insulation which is indicated by its chemical and physical changes [21]. A decrease in mechanical strength is attributed to decrease in the number of glucose units in molecular chain (DP) [22].

2.5.2 Thickness of Paper

Thickness of insulation paper varies in the range of $75-250$ micrometers [18]. Using thick and dense paper increases dielectric strength of the insulation but reduces its heat transfer capability from conductor windings to the circulating oil. Therefore, there is a compromise between these two parameters that determines an optimum thickness in the design process.

---

[1] In both references [1], [18] the cellulose formula has been misprinted as $(C_5H_{10}O_5)_n$. The original paper [3] shows the correct form of $(C_6H_{10}O_5)_n$.

Also, to optimize dielectric strength of insulation, layering of paper is very common for wrapping the conductor [1].

2.5.3 Physical Changes in Paper

Physical structure of paper contains many micro-scale cracks in different regions of the fibers. It has been understood that by increasing ageing time, the cracks develop further [4], [20]. These cracks eventually reduce mechanical strength of the paper, determined by tensile strength index. Cracks are rarely visible with regular optical microscopes but the imaging performed by Scanning Electron Microscopy (SEM) clearly shows the progressive development of cracks due to ageing [6].

2.6 Life Expectancy of Power Transformer and Time of Ageing

As a rule of thumb, life-time of a transformer is estimated based on the life-time of its solid insulation. Under normal operating conditions[1], the minimum life expectancy of a power transformer is 180,000 hours (20.5 years). However, in practice they are expected to be in service for about 30 years [1]. Based on statistics in [23], power transformers with operational life of over 30 years are less than 5% in China which decreases to less than 1% for

---

[1] Ambient temperatures in the range of -20 ºC to 40 ºC, altitudes lower than 1000m, and no overload or seismic condition [1].

transformers with 40 years of service. Life-time of a power transformer in hours can be estimated from[1]

$$Life = e^{\left[\frac{B}{T+273}-A\right]},$$ (2-1)

where A and B are constants based on measurements and T is the ageing temperature in °C. For example if we assume $A = 29$, $B = 17{,}749$ based on the calibration test results example in IEEE C57.100-2011 standard, with ageing temperature of 180°C[2], the expected life is 26,397 hours or 3 years. Equation (2-1) shows that ageing temperature has a significant impact on life-time where increasing ageing time decreases life expectancy of the power transformer.

2.7 Importance of Condition Assessment of Power Transformer

As mentioned earlier, neglecting cooling fans, usually there are no mechanical moving parts in the insulation system of a power transformer and the main limiting factor for the life expectancy is its insulation lifetime which mostly depends on thermal ageing of oil-paper combination. Therefore, it is important to have an estimate of the insulation lifetime based on the current condition of the transformer. In this research, we are more interested in

---

[1] Based on IEEE.C57.100-2011 (STANDARD Test Procedure for Thermal Evaluation of Insulation Systems for Liquid-Immersed Distribution and Power Transformers).

[2] This temperature is chosen based on section "A.2 Test temperatures and test periods" of IEEE.C57.100-2011 standard as an example, however it is not a normal operating temperature for the transformer.

physical changes of paper insulation due to ageing time and temperature[1]. Classification of paper samples based on different ageing levels will provide the potential to estimate life-expectancy of the power transformer and scheduling timely maintenance before disastrous transformer failure occurs.

2.8 Problem Definition

Common problems of oil-immersed power transformers can be categorized as: a) manufacturing defect related problems such as cooling problems and winding/insulation quality, b) ageing/deterioration related problems such as thermal ageing of insulation material, and c) operating conditions related problems such as overloading.

Deterioration in oil-immersed power transformers usually is accompanied with signs such as decrease in mechanical strength of paper insulation material, sludge and/or sediments in oil. Deterioration of insulation material is mainly due to ageing phenomenon. Ageing may accelerate in the presence of different stress sources such as voltage stress, mechanical stress, and thermal stress. It is well understood that thermal stress plays an important role in ageing process [22].

High temperature has a deteriorating effect on chemical structure of the cellulosic paper insulation. The deterioration in paper affects the physical structure of its compounding

---

[1] We have considered ageing phenomena with a macroscopic viewpoint; therefore neglecting details of microscopic chemical reactions or effect of the circulation of oil on the roughness of paper.

fibers which is not visible with naked eye. High temperature in presence of moisture or water content of paper in the transformer also could result in gas bubbles in the liquid insulation (oil) which reduces dielectric strength of the oil and causes failure. In fact, not only high temperature of above 120 degree affects insulation material, but also mid-temperature (100 degree) in long-term can have the same undesired effect on insulation material. Degradation and deterioration of insulation are advanced stages of ageing.

Ageing related problems can cause short-term or long-term failures in power transformers. Early replacement of insulation material, if possible, is not economically advisable which can also be time consuming. On the other hand late detection of insulation problem causes equipment loss and/or damages to the transformer. Therefore, using proper condition monitoring techniques, whether online or offline, remote or *in-situ,* in a timely manner, saves time and budget resources.

2.9 Existing Solution - Current Testing Methods, and Their Limitations

Various diagnostic tests for condition assessment of power transformers have been proposed and reviewed in the literature [16], [20], [24]–[26]. Major test routines recommended for power transformer condition assessment can be classified as:

-   Chemical tests; such as Degree of Polymerization (DP) measurement, Dissolved Gas Analysis (DGA), and Furan Analysis [20], [25],

- Physical tests; such as oil quality assessment to determine water content, acidity, viscosity, dielectric strength, etc [4].

- Electrical tests such as Partial Discharge (PD) detection, Dielectric Loss (Power Factor) measurements, and Frequency Response Analysis (FRA)[26] .

Among these tests, chemical tests are very common to address issues with the solid insulation. Here a brief review of these methods is presented as recommended in the industrial standards [27].

2.9.1 Measurement of Degree of Polymerization (DP)

DP measurement is a direct indication of paper degradation in transformers, cables and capacitors. DP rapidly decreases due to ageing especially in the presence of high temperatures, oxygen, and moisture. Standard test procedure for obtaining DP based on viscosity of a solution of paper in specific chemical reagent is defined in ASTM-D4243[1] or IEC60450[2] standards equivalently. As stated before, DP indicates average number of glucose units composing cellulose polymer which also has been correlated to mechanical tensile strength of paper fibers. Non-aged kraft paper has a DP value of over 1000. Based on a criteria from previous published works [28], a transformer with aged paper insulation is

---

[1] ASTM D4243 - 99(2009); Standard Test Method for Measurement of Average Viscometric Degree of Polymerization of New and Aged Electrical Papers and Boards.
[2] IEC60450; measurement of average viscometric degree of polymerization of new and aged cellulosic electrically insulating materials.

assumed at the end of its useful operational life if a 50% reduction in its tensile strength, corresponding to a DP value of less than 400, occurs. Paper insulation in a transformer with DP of 200, has lost 70% of its mechanical strength. Also, it has been reported that DP in the range of 150-200 corresponds to a loss of 80-percent of mechanical strength of the paper insulation [29].

2.9.2   Dissolved gas analysis (DGA)

Various dissolved gases in the transformer oil such as Nitrogen (N_2), Oxygen (O_2), Hydrogen (H_2), Carbon dioxide (CO_2), and Methane (CH_4) are detectable in this method based on "gas chromatography". The aforementioned gasses are considered as the key elements in transformer oil dissolved gas analysis. Each of them corresponds to a pre-dominant source of ageing as listed in Table 2.1.

Table 2.1 Typical gases in the oil tank of a power transformer in fault condition[1].

	Gas	Origin
CO	Carbon monoxide	- Ageing of Cellulose (heat-accelerated) - Air Pollution
CO_2	Carbon dioxide	- Ageing of Cellulose (heat-accelerated) - Air Pollution
CH_4	Methane	- Overheated oil (adjacent to hot metal) - Partial Discharge
H_2	Hydrogen	- Overheated oil (adjacent to hot metal in the core or winding) - Partial Discharge

---

[1] Based on the C57.140-2006 - IEEE Guide for the Evaluation and Reconditioning of Liquid Immersed Power Transformers.

DGA test is performed on a routing basis to determine sources of the transformer fault in the laboratory and is very common for transformer assessment.

2.9.3 Furan analysis

Degradation of cellulose in the paper is accompanied with production of aromatic chemicals. 2-FurfurALdehyde (2-FAL) is the most stable furanic compound known as an indication of the sole paper degradation not oil. It is also a routine test to detect overheating of the cellulose. Standards such as ASTM D5387 addresses the test procedure.

2.9.4 Limitations of current testing methods

Not all of the aforementioned test routines in the standards are specifically designed for assessment of solid insulation. Some of them can give an estimate of the solid insulation condition. Major limitations of current chemo-metric test can be summarized as follows.

2.9.4.1 Limitations of Degree of polymerization (DP) Measurements

In order to collect samples for DP tests, the paper should be collected from locations that have the most rapidly aged paper. Once a transformer is manufactured, the paper with the highest probability of becoming weakened is usually in locations that cannot be easily accessed without risk of damaging the transformer. As a result, collecting the paper samples from a transformer may jeopardize the reliability of the transformer. For in-service equipment, taking samples must be limited to areas that after repair will result in a

negligible increase in the probability of failure as a result of the paper sampling. Locations are selected based on an individual's judgment, but should usually be in the upper part of the transformer where the oil temperature is the highest. A coil lead or a crossover connection is a typical location for taking a paper sample. Collection of samples that are directly in contact with the conductor is important. If the transformer oil has been exposed to air, the outer layer of the paper should also be tested. Obtaining a sample of paper in contact with the conductor often requires the removal of a considerable amount of insulating material. It is important that the insulation be carefully removed and the location and layer from which the paper was removed be documented. The repair of the insulation system requires great care. For example, paper tapes must be properly applied to replicate the original insulation. Often, paper tapes should be pre-impregnated with clean dry oil. The common concept that "more paper is better" is a poor idea as excessive paper can cause hot spots by restricting the cooling of the conductor. It is recommended that properly trained personnel repair disturbed sections of the insulation system. Unfortunately, for most transformers that are in service, the results of DP tests may not be a representative of insulation that is in a higher state of deterioration.

2.9.4.2 Limitation of Furan Method

Furan compounds will change in content during each oil processing of the transformer. Therefore, furan compounds cannot be a proper measure between periodical tests. It is an

indirect measure of ageing of paper which has less accuracy in comparison with DP measurements.

2.9.4.3 Limitation of DGA:

Similar to furanic content test, there is a probability of not detecting dissolved gasses in oil when they change rapidly between normal test periods. For more accurate results, the test should be carried out in the laboratory with enough samples to provide reliable feedback of cellulose condition in the power transformer. In general, performing more tests will be costly and impractical.

As closing remarks on the limitations of current insulation testing methods, we should mention that optical-based methods are not as developed and as well-established routines, although there do exist spectroscopy measurement methods, thermography of transformer with Infra-Red (IR) camera and online temperature sensors based on optical fibers. In the next chapter we will focus on the optical speckle phenomena and its potential application for classifying aged papers.

Chapter 3

Optical Speckle

3.1 Introduction

The word "speckle" in general means "a small mark of color" like brownish spots on a ripe banana or a night sky full of stars. Shortly after the invention of the laser in the early 1960s, the term "speckle" was used widely to describe the optical phenomenon associated with grainy intensity patterns due to self-interference of light [9]. In fact speckle phenomenon was mentioned by Isaac Newton in the 18th century and later by other scientists such as Exner, Von Laue and Le duc de Chaulnes in early 19th century. They discovered a close relationship between interference of light waves and the speckle phenomenon. The later introduction of laser sources, resulted in an in-depth understanding of this concept [30], [12].

By illuminating an object with a monochromatic light source such as a laser, due to the coherence of light waves, visible reflected or transmitted waves can produce non-vanishing interference patterns from their interference. This mutual interference of light results in a pattern with bright and dark regions, corresponding to the maximum and minimum of the resulting interference pattern. This interference pattern is a function of the random fluctuations in light scattered from the object, the wavelength of light, the geometry of

illumination and the detection method. Figure 3.1 is a schematic diagram of the direction

of the incident illumination and randomly back-reflected light waves.
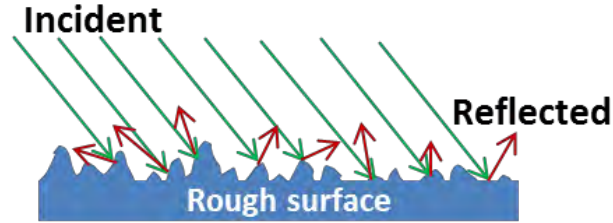
Figure 3.1 Illumination of a surface by plane monochromatic (coherent) light. Back reflected waves have random directions which depend on the surface roughness.

If random surface or volume fluctuations of the illuminated sample are comparable to the

wavelength of illumination, e.g. rough surface of paper, the interference pattern will be in

the form of randomly distributed bright and dark spots called a speckle pattern [31], [32].

Figure 3.2 shows a typical speckle pattern captured from surface of a sample of karft paper,

in which randomly distributed bright and dark spots are clearly visible.
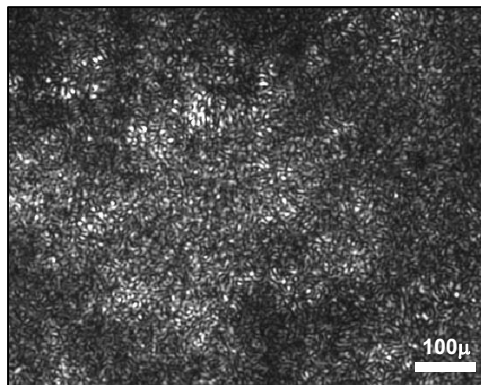
Figure 3.2. Optical speckle pattern from an aged kraft paper sample, taken with 10× objective lens focused to a CCD camera.

3.2 Origin of Speckle

We can interpret a speckle pattern as a random interference pattern. The interference of light is closely related to the wave nature of light. Here a brief review of interference as the origin of speckle is presented. Based on the wave theory of light, light propagates as waves that can be represented by a real function of position and time. In the especial case of monochromatic illumination, this wave is a single frequency function of time that travels a distance equal to its wavelength in each time cycle. With this simplifying assumption of a pure monochromatic (single frequency), the real wave-function can be written as

$$u\,(r,t) = a(r)\cos[2\pi vt + \varphi(r)], \tag{3-1}$$

where $a(r)$ = amplitude, $\varphi(r)$ = phase, v = frequency (cycles/s or Hz.

Optical frequencies are in the range of 3×10^{11}Hz to 3×10^{18} Hz, where visible light frequencies are between 1.3×10^{15}Hz (760 nm, red) to 1.8×10^{15}(390 nm, violet). For a monochromatic laser beam, it is usually easier to represent $u\,(r,t)$ in a phasor form:

$$u\,(r,t) = Re\{U(r,t)\} = \frac{1}{2}[U(r,t) + U^*(r,t)], \tag{3-2}$$

Where

$$U(r,t) = a(r)\exp[j\varphi(r)]\exp(j2\pi vt). \tag{3-3}$$

Defining $U(r) = a(r) \exp[j\varphi(r)]$ as the phasor of wave-function of light, we get

$$U(r,t) = U(r) \exp(j2\pi\upsilon t). \tag{3-4}$$

$U(r,t)$ is known as the complex wave-function[1] and $U(r)$ is the complex amplitude or phasor representation of the light wave rotating with angular velocity of $\omega = 2\pi\upsilon$ rad/sec due to the $\exp(j2\pi\upsilon t)$ term. Usually optical detectors such as CCD sensors or human eyes are sensitive to the intensity of light rather than its complex amplitude containing the phase term. Therefore it is useful to convert the complex amplitude to optical intensity. The optical intensity is defined as [33]:

$$I(r) = |U(r)|^2 \tag{3-5}$$

Now consider two monochromatic waves with the same frequency (color) and phasors $U_1(r)$ and $U_2(r)$ that are reflected from or transmitted through an object. Under the simplifying assumption that the two waves are propagating in the same direction having the same linear polarization, the resultant amplitude of the superposed wave will be given by

$$U(r) = U_1(r) + U_2(r). \tag{3-6}$$

The resulting intensity could be written as

---

[1] Recalling that we defined $u(r,t)$ as the real wave-function.

$$I = |U|^2 = |U_1 + U_2|^2 = |U_1|^2 + |U_2|^2 + U_1^*U_2 + U_1U_2^*$$

$$I = \left\{ |U_1 = \sqrt{I_1}\exp(j\varphi_1)| \right\}^2 + \left\{ |U_2 = \sqrt{I_2}\exp(j\varphi_2)| \right\}^2 + U_1^*U_2 + U_1U_2^*$$

$$I = I_1 + I_2 + 2\sqrt{I_1I_2}\cos\varphi$$

(3-7)

where $\varphi \triangleq \varphi_2 - \varphi_1$. Equation (3-7) clearly shows that the intensity of the sum of two monochromatic waves depends on the difference between their phase angles. This phase difference could be due to a difference in their optical path lengths when they arrive at the optical detector. According to (3-7), in the constructive interference case, the brightest intensity will be recorded on the detector when $\cos\varphi = 1$. In the destructive case, the weakest intensity will be recorded when $\cos\varphi = -1$.

Now consider the general case of addition of multiple monochromatic waves with random amplitudes and random phase differences. The resulting intensity pattern will be a random distribution of bright and dark regions on a screen or a detector, thereby forming a speckle pattern, as shown in[30], [34].

Dainty [30] and Goodman [35] have thoroughly investigated and classified both the propagation and statistics of the speckle phenomenon in two different configurations of free-space light propagation, *i.e.*: Light propagation without any guiding lenses (known as objective speckle), and light propagation via an imaging system including lenses (known as subjective speckle). Each propagation scheme can also be considered in either transmission

or reflection modes, depending on the relative positions of the illumination, the object and the detection screen[1].

The mathematical descriptions of speckle patterns typically have complicated statistical properties. Goodman modeled optical speckle as a superposition of a very large number of phasors, whose resultant undergoes a random walk in the complex plane. He also showed that in the special case of polarized light, the optical intensity of speckle[2] at a single point in space follows a negative exponential probability density function (PDF) given by [30]

$$P(I) = \frac{1}{<I>} \exp(\frac{-I}{<I>}), \qquad \text{(3-8)}$$

where $<I>$ is the mean (average) intensity. The PDF in (3-8), (see Figure 3.3) shows that the most probable brightness value is zero. This means that dark regions are more likely to occur than bright regions which is also apparent in the general pattern of Figure 3.2.
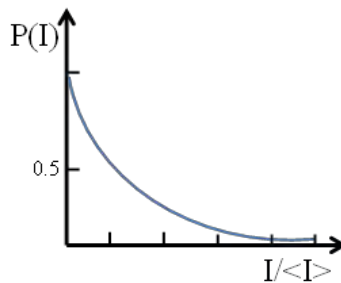
Figure 3.3 Probability of intensity (brighness) of a fully developed optical speckle, adopted from [30].

---

[1] In this project we have considered reflection and transmission modes in the imaging configuration.
[2] Also known as fully developed speckle, sec 3.2.1 p. 28 of [35].

Another parameter to characterize the optical speckle is the *speckle size*, which is defined as the center-to-center distance of adjacent dark spots, or adjacent light spots, that are present in the speckle pattern. Speckle size is related to the characteristics of the imaging system (such as wavelength of illumination and objective magnification) and usually is not an inherent property of the sample under investigation. In this project we have not considered this parameter as a major contributing factor since there is possibility of implementing the optical setup with different imaging characteristics which results in different speckle sizes that are not solely dependent to the physical properties of the paper samples.

3.3 Effect of Coherence of Light on Speckle Formation

Coherence of light can be described as the ability of its wave functions to interfere with each other. Laser illumination is considered more coherent that sunlight since it can preserve its characteristics (amplitude and phase) for larger distances (spatial coherence) or longer duration of time (temporal coherence) with regard to the wavelength of light. As an example, coherence time of a well stabilized laser could be in the order of 10^{-4} seconds with coherent length of about 30 km while for the filtered thermal light (from a light bulb) coherence time reduces to 10^{-8} seconds and coherence length will be in the order of 3 meters.

Coherent waves can interfere with each other to produce very distinct bright (constructive) and dark (destructive) interference patterns. Interference pattern of partially coherent light

waves is not as clear as coherent waves; non-coherent light waves, theoretically cannot interfere. But in realty since interference is a mathematical addition of waveforms, waves always can add to each other however in the case of non-coherent or partially coherent waves, the resulting pattern will not be a clear interference pattern. For example, the sun is usually considered as an incoherent light source but it still has enough coherence to form speckle on the microscope, depending on the aperture[1] of the optical setup. [36]

Since speckle formation is closely related to the interference of light, in a sense, more coherent light can produce more speckle; but this does not mean that non-coherent light will not produce any speckle. In fact for the less coherent light, if we add different propagating wave-functions to find the final interference pattern, the outcome will be a less distinguishable interference pattern; since the bright and dark regions cancelling out each other after summation on a large scale. According to Section 1.10 in [12][2], any white light source which is illuminating an object may produce a speckle pattern if the surface of the object is covered with proper reflective coating.

---

[1] Aperture can be defined as "the opening that determines the cone angle of a bundle of rays that come to a focus in the image plane" in optics [36].

[2] Under title "white light speckle".

3.4 Applications of Optical Speckle

On examining the scientific literature for optical speckle, we can distinguish two different point of views on its nature and how it should be approached. One view is to consider speckle as a form of noise which degrades imaging quality, therefore minimizing its effect is the final goal. This approach is usually identified by keywords such as "speckle reduction" or "speckle suppression". Speckle reduction techniques in laser based imaging, e.g., optical coherence tomography (OCT) have been investigated in the literature [35], [37], [38]. The other point of view is to consider speckle as a "signal" rather than noise which conveys useful information. Applications of optical speckle as a useful information carrier in metrology, signal coding, astronomy, measurement of deformation and shape, flow detection, displacement measurement, vibration analysis by Electronic Speckle Pattern Interferometry (ESPI), paper fingerprinting for authentication and more have been extensively described in the literature [10], [12], [31], [32], [35], [39], [40]. In this thesis, we will consider optical speckle as a source of information about the structural properties of kraft paper.

3.5 Other Methods to Characterize Paper Properties

Paper properties include color, glossiness, ink absorption, porosity, compressibility, mechanical strength, roughness, etc. Roughness is one of the most researched surface features of the paper that characterizes the unevenness of the paper surface. Paper roughness

measurements in the paper industry are usually based on the measurement of air leakage through paper. This method, known as the *Bendsten Method,* is a non-optical and invasive method that damages the paper sample during measurement. Regarding optical methods, in general they have been used for investigating paper properties for quality assurance purposes in the paper industry; such as using optical profilometers and glossmeters. Spectroscopic methods, Scanning Electron Microscopy (SEM) imaging, and confocal microscopy have also been used to investigate paper [6]. Alarousu in [5] investigated application of Optical Coherence Tomography (OCT) for 2-D and 3-D imaging of paper for applications related to the forestry industry in Finland. Also considerable research has been conducted to characterize surface properties and topography of paper, *e.g.,* work by A.Teleman *et al.* in Sweden that uses a Confocal Laser Scanning Microscope (CLSM) to image topological changes of paper due to compression [7]. But as the best of author's knowledge, there has been less attention for using optical speckle in the power transformer industry. The optical speckle based techniques are mainly used to measure paper roughness. In one of the significant researches in this field, Abdiel *et al.* used a limited number of statistical surface texture features of speckle patterns resulting from paper to investigate its surface roughness [41]. They compared their optical speckle-based results with the Bendsten air leakage-based method and showed high correlation between non-optical and optical techniques. Their work validates using optical speckle-based methods as a non-contact and

possibly real-time method to measure paper roughness [10], [41]. In another related work by Nicklawy *et al.* paper roughness has been characterized by optical speckle patterns during paper displacement [42]. Most of the studies to characterize paper using speckle patterns measure its roughness using the correlation between two successive speckle patterns obtained by changing the direction of illumination or the wavelength of the laser source [12]. Those techniques are basically based on the speckle interferometry with the goal of detection of displacement or deformation in each sample [9]. In this thesis, speckle interferometry has not been used; instead a fixed illumination direction and wavelength have been employed to capture speckle patterns, which results in a simple measurement setup in comparison to the aforementioned techniques.

Chapter 4

Methodology and Experiment Setup

4.1 Hypothesis

The hypothesis of this project is to verify that the physical changes in the fiber structure of the kraft paper, due to thermal stress during ageing, are distinguishable by processing of the speckle patterns. In this regards, we changed the duration of exposure of paper samples to the thermal stress while setting the temperature to a fixed value. We expect physical changes in paper samples with different ageing levels, affect the speckle pattern of each sample differently.

4.2 Methodology

The proposed methodology and experiment includes: a) Preparation of samples with different ageing levels by performing accelerated thermal ageing, b) Acquisition of speckle patterns using the proposed optical setup, and c) Image processing including feature extraction and classification. Paper samples with different ageing levels are prepared and images of their speckle patterns are acquired. To simulate actual thermal ageing process of paper in a transformer, we used an accelerated thermal ageing procedure to mimic the thermal ageing phenomenon in a much shorter time in the lab environment.

4.3 Preparation of Accelerated Thermal Ageing Samples

We used brand new Kraft paper[1] and transformer mineral oil[2] that has been impregnated

with transformer oil in the experiments. The Kraft paper were cut in 1 cm × 3 cm rectangles

to fit in 25 ml, 3 cm × 6 cm glass vials of mineral oil[3]. Figure 4.1 shows a schematic of the

setup for preparation of thermally aged paper samples.
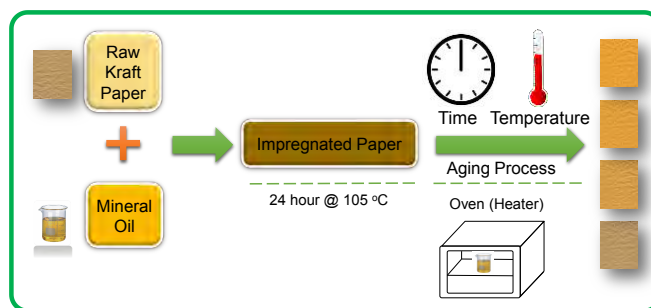
Figure 4.1 Accelerated thermal ageing setup diagram; impregnation of Kraft paper is performed by mineral oil in the oven for 24 hours at 105°C, afterwards oil-impregnated samples were exposed to 140°C for accelerate thermal ageing for 120, 240, and 400 hours.

Each paper sample was weighed with a calibrated scale before and after the accelerated

thermal ageing process. To remove moisture from the samples, we placed them in the oven

at 105°C for 24 hours. Weighing afterward indicated weight reduction of each sample due

to evaporated water from it. Accelerated ageing is a common technique [43] to age samples

---

[1] The author is thankful to CG Power Systems Canada for providing the paper samples.

[2] Assistance of Nathan Jacob for providing oil supplies and support from Manitoba Hydro High Voltage Test Facility (HVTF) are acknowledged for conducting the accelerated thermal ageing process.

[3] Different brands of mineral oil with specific grading according to the standards are available for transformer oil such as Luminol (by Petro-Canada) [55] , Voltesso 35 & Voltesso N36 (by Mobil) [56], Envirotemp FR3 (by Cargill) [53]. Chemical properties such as viscosity & pour point, in line with electrical properties such as Dielectric Breakdown Voltage are important factors in choosing proper insulating fluid according to the operational condition of the transformer. In this project VOLTESSO™ 35 and LUMINOL oils were used which are commonly used in the power transformers in the Manitoba.

(here kraft paper) under thermal or electrical stress which has been mentioned in the related literature [44], however to the best of the author's knowledge there is no standardized test procedure to age kraft paper in the transformer oil. In the next step, we filled the vials with mineral oil. The samples were sealed and divided in $1 + 3$ groups. The first group of samples was kept in ambient room temperature as control (reference) samples without ageing. We placed the 3 remaining groups of samples in the oven at $140°C$ for 120, 250, and 400 hours, respectively. Under controlled lab conditions, samples were removed from the oven and transferred to the Computational Imaging Laboratory at the University of Manitoba. Figure 4.2 shows oil vials containing kraft paper samples with different ageing levels, in addition to the microscope slides preparation process.

(a)   (b)

(c)
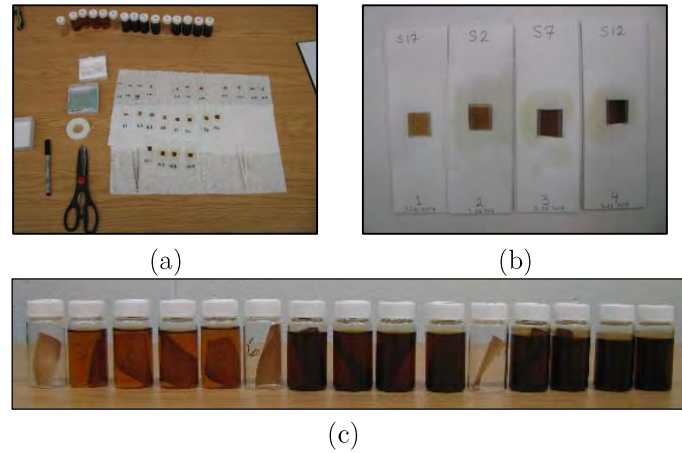
Figure 4.2. Preparation of oil-impregnated paper samples in (a), prepared samples on manually built slides (b) and original vials containing oil and/or paper in (c). Note that the more aged samples are visibly darker in color (b) in paper, and (c) in oil from left to right.

The largest field of view in the experiments with the Olympus IX73 microscope, using a 10x objective lens, is 0.8 cm × 0.8 cm, therefore the minimum size of each paper sample was

chosen to be greater than the field of view of our imaging setup, *i.e.* for each class of aged paper, we cut the paper in 1cm × 1cm squares. We used 25 mm × 75 mm microscope slides and 25mm × 25mm cover slides to place the paper samples on the microscope's translation stage (slide holder). As the area of each sample was 100 mm^2 (=10mm × 10mm) and the microscope's field of view for 10× objective lens was 1 mm^2, we were able to capture at least 50 images per sample in each class of ageing.

4.4 Optical Measurement Setup

We developed the experimental setup using two basic measurement modes: reflection and transmission (see Figure 4.3). A laser source illuminates the object's (paper sample) surface. Monochromatic light waves, superimposing with one another just after interacting with the sample's surface, are focused by an objective lens on a CCD sensor, where a speckle pattern is recorded.
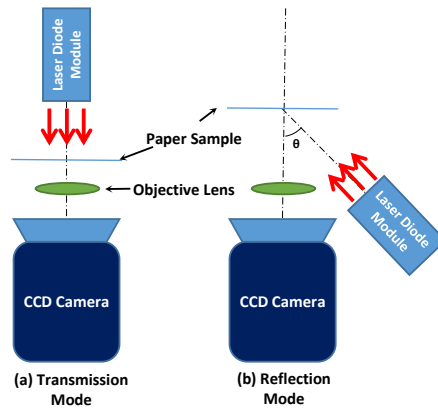
Figure 4.3. Schematic setup of speckle image acquisition in (a) transmission and (b) reflection mode.

4.4.1   Stand-alone Optical Speckle Acquisition Setup

The stand-alone optical speckle acquisition configuration is a classic setup to acquire optical

speckle in reflection mode [12], [30], [35]. The following is a description of this setup. On a

60×60 cm optical table (also called breadboard), a 655nm, 5mW red laser diode with

collimated beams illuminates the paper sample with an angle of $\theta = 25°$ which is installed

on an optical platform[1]. The optical speckle pattern from the paper sample is captured by

the Retiga 2000R CCD camera (see Figure 4.4).
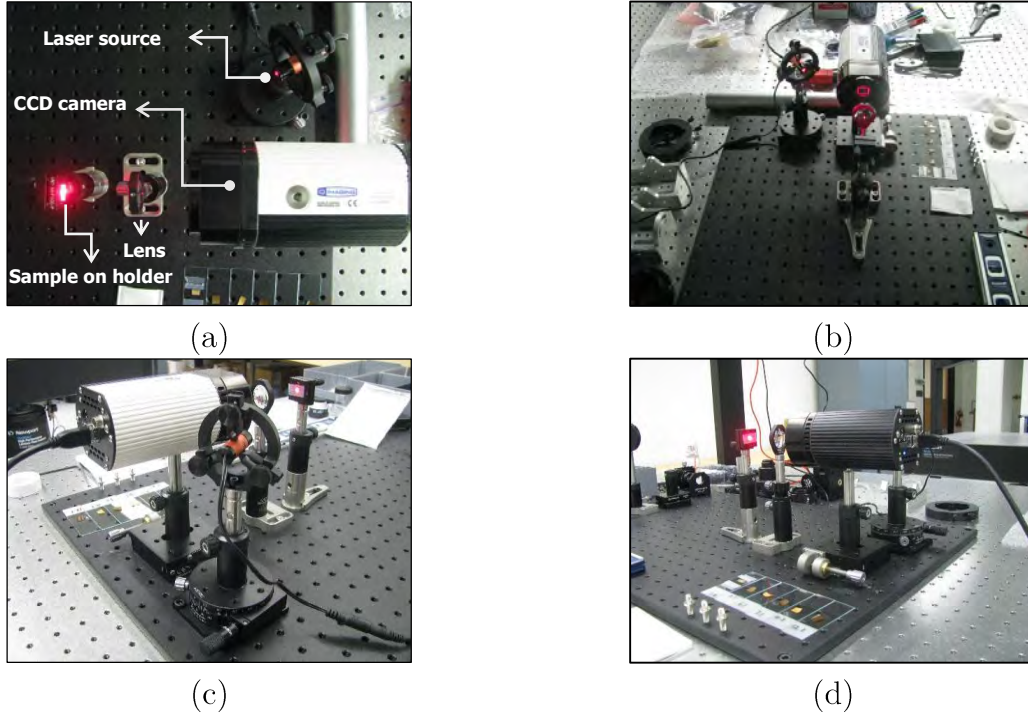
Figure 4.4. Speckle acquisition setup; (a) top view showing laser source, CCD camera, converging lens, and illuminated sample, (b) front view of the system, (c) and (d) side views.

Part-list of the required components for this setup have been provided in Appendix B.

---

[1] In similar reported projects, laser source with 632.8 nm with an angle of 15° in [41] and 11° in [10] (measured from the normal axis to paper surface) has been used.

4.4.2   Microscope-based Optical Speckle Acquisition Setup

Another optical setup was developed on the frame of an Olympus IX-73 inverted microscope. Earlier efforts to use a microscope to magnify speckle patterns recorded on photographic plates (negative film) has been reported in [12]. The advantage of using microscope is that it facilitates image capturing with more accurate focusing mechanism and less mechanical displacement concerns during sample scanning. In addition, the acquired speckle pattern from the sample will be magnified by the microscope. Focusing and alignment is handled by using the focusing knob of the microscope, in addition to the fine focusing knob with a resolution of 1μm, that allows adjustments of the vertical distance between the objective lens and the CCD camera which is connected to the bottom port of the microscope (see Figure 4.5 a). Also the built-in translational stage of the microscope which is basically a sample holder, provides a mechanically reliable and stable platform for our paper samples. This stage allows convenient displacement of the sample in a horizontal plane (XY plane) perpendicular to the microscope's vertical optical axis (Z axis). The following is the description of reflection and transmission mode setups on the microscope. In these configurations, the standard illumination source of the microscope is not used.

4.4.2.1   Microscope-based Experimental Setup - Reflection Mode

In this configuration, the laser source illuminates the paper sample from the side and the reflected light is focused by the microscope on the CCD camera as shown in Figure 4.4b,

Figure 4.5, and Figure 4.6. To implement this setup, some modifications to the microscope were needed. A 60×60 cm aluminum optical bread-board was machined and installed between the microscope and the supporting metal poles, as shown in Figure 4.5. The bread-board provides enough room to place the laser source.

(a)

(b)

(c)
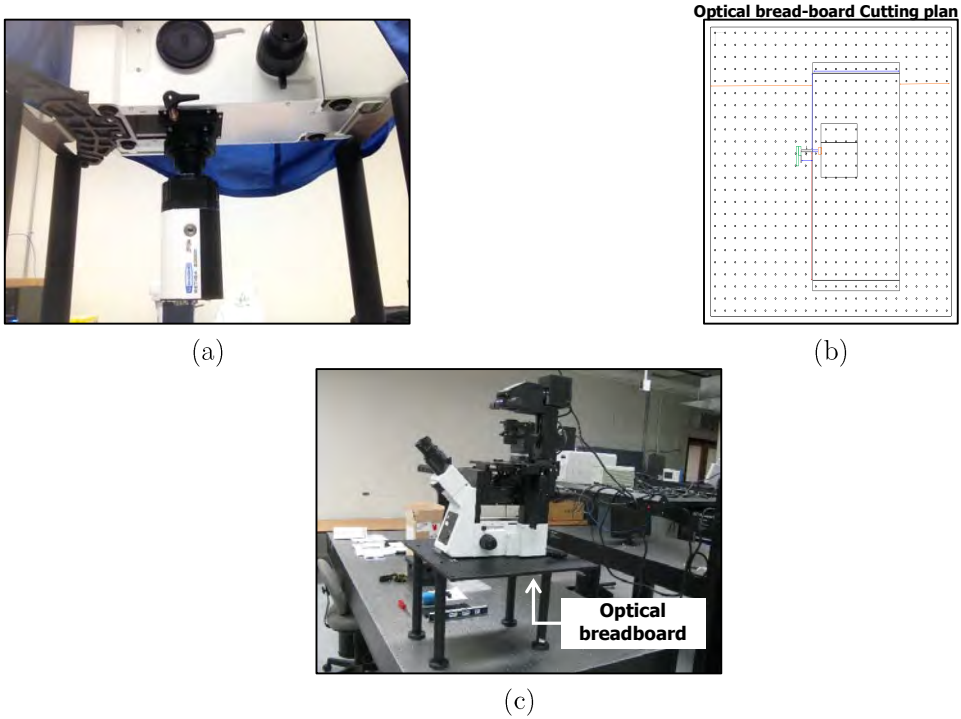
Figure 4.5. Breadboard placement, (a) shows the bottom port of the microscope, (b) cut design of the optical breadboard to fit beneath the microscope, (c) shows Olympus IX-73 microscope after breadboard placement.

The laser source, installed on an angled bracket with $\theta = 45°$, illuminates the sample from the side. The light along the optical axis of the microscope is captured as an optical speckle pattern on the CCD camera which is installed on the bottom port (see Figure 4.6).

(a)

(b)

(c)
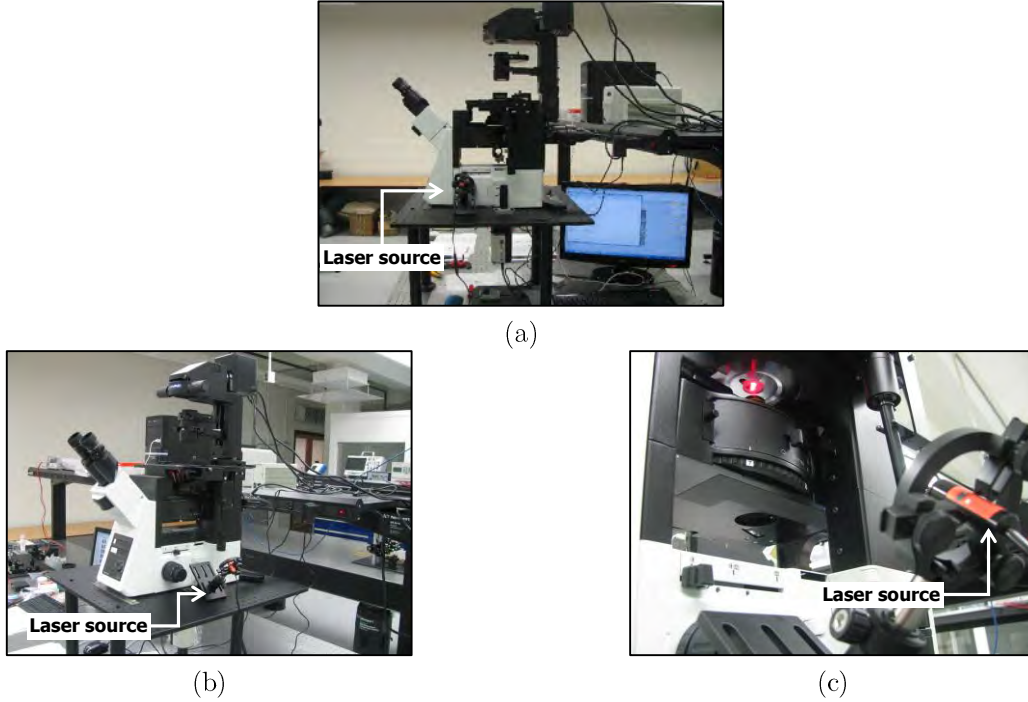
Figure 4.6. Reflection mode speckle setup on the Olympus IX-73 microscope; (a) and (b) side views of the microscope after installing the optical bread-board platform and laser source, (c) shows a closer view of the laser source aimed toward the sample stage.

To minimize the noise effect of undesired stray light reflecting from surrounding objects, the original light path of the microscope was blocked by an opaque slide attached to the sample (see Figure 4.7).

<table>
<tr><td>(a)</td><td>(b)</td></tr>
</table>
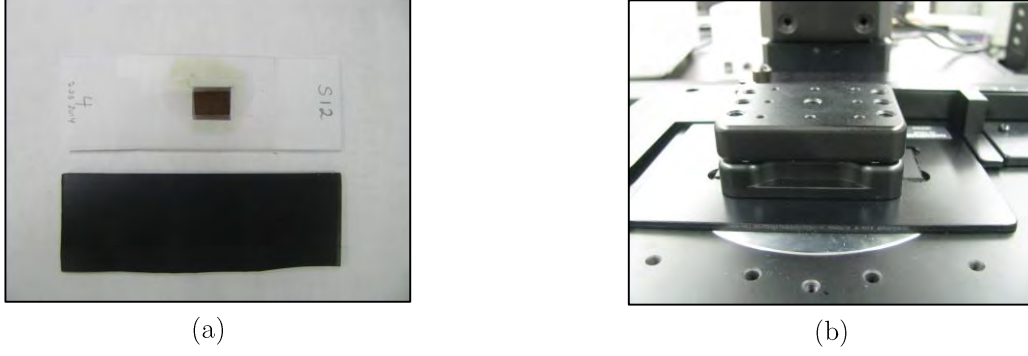
Figure 4.7. (a) Paper sample on a hand-made light-blocking slide (b) fixing the slide on the microscope stage.

4.4.2.2 Microscope-based Experimental Setup - Transmission Mode

Since our paper samples are very thin (approximately 100 micron) and oil-impregnated, they are transparent to the microscope's visible laser illumination. This transparency allows us to obtain relevant optical speckle patterns in transmission mode, which need the light to pass through the sample. In transmission mode, the laser illumination is perpendicular to the sample. Two optical mounting posts (Newport SP6, Newport SP8) are attached together via a right-angle post clamp (Newport CA-1) which is connected to a universal fixed lens mount (Newport AC-1A). The aforementioned opto-mechanical structure is installed on the platform provided by the microscope's translation stage; no other modifications to the microscope are needed. The reflection mode setup based on the microscope is showed in Figure 4.8. A detailed parts list is provided in appendix B.

| (a) | (b) |
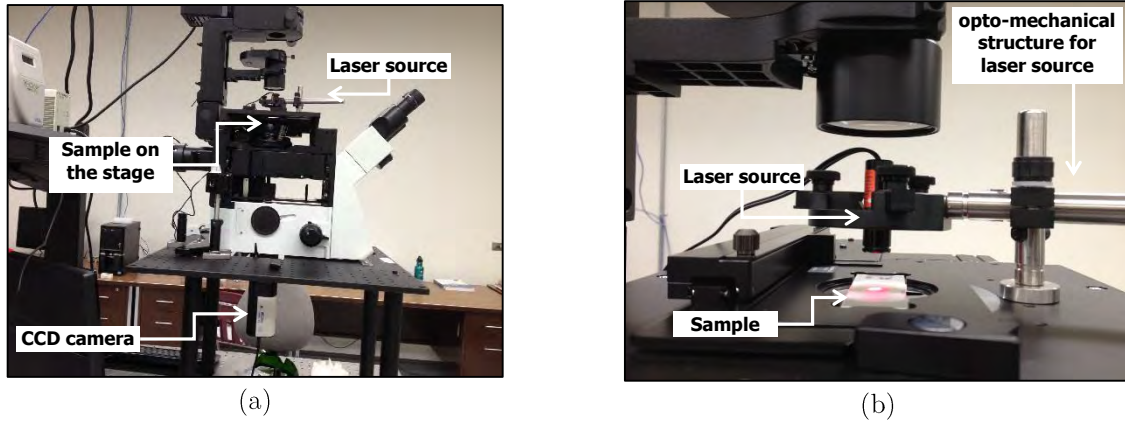
Figure 4.8. The transmission mode experimental setup (a) and a closer side view in (b), installed on the IX73 Olympus microscope.

4.5 Image Acquisition Settings

To acquire images of the paper samples, a Retiga 2000R CCD camera with internal cooling was used. For importing these images to a PC, Q-Capture Pro 7 software was used. Specifications of the imaging setup are summarized in Table 4.1.

Table 4.1. Imaging setup specifications

Item	Description
CCD Camera	Retiga 2000R, C-Mounted on IX73 Olympus (inverted type microscope)
Pixel size	0.7 μm
Laser source	655nm, 5mW Red Laser Diode Module 13x42mm, Collimated w/ AC.
Capturing Software	Q-Capture Pro7
Bit Depth	16 bit
Image size	1600 x 1200 pixels
Objective Lens	10x, UIS2, LMPlan N, f=18mm (focal point)
Exposure time	1 ms (transmission mode), 25 ms (reflection mode)
Imaging Device	IX73 Olympus inverted type microscope

4.5.1 Remarks on the Experimental Setups and Imaging Process

The laser source in our experiments was a basic semiconductor red laser pointer. The main benefit of this selection is its ease of use, compactness, good thermal properties and low cost. A simple semiconductor laser is less expensive than a typical He-Ne gas laser. Also for industrial applications, a semiconductor laser is more practical to use, compared to gas based lasers that have been used in other areas of research [10], [41], [42]. In order to acquire more reliable data, the following issues were considered during the measurement and imaging processes:

- **Avoiding de-focused image regions**: Using a high magnification, e.g., 40× objective lens in a microscope, is inherently accompanied with lower depth of focus. Therefore, the potential of having "out of focus (de-focused) image regions" increases. We used two remedies to overcome this problem: First, we used a 10× objective lens, instead of a higher magnification one, which considerably reduced de-focused image areas. Second, the sample should be placed as flat as possible on the translation stage. We used a 25 mm × 25 mm glass cover slip and regular tape to secure the paper sample on the microscope slide to be used in transmission mode. For reflection mode, the paper sample was attached directly to the light blocking slide. To further reduce de-focusing issues, some image processing methods such as EFI (Extend Focal Imaging) could be used [45].

- Care taken while performing the measurements: The forceps and scissors were cleaned prior to each cut of the paper sample to prevent mixing oil from different samples while cutting them. Gloves were used to prevent any fingerprints on the oily paper samples and measuring instruments. All the samples were marked properly and the acquired data were recorded using time tags and sample tags. We stored all the sealed samples in their appropriate containers that was included with moisture absorber (silica-gel) packs. The vials had tight sealed lids to prevent change to the moisture content of the samples. The used optical parts including lenses, CCD camera sensor, microscope stage, and slides were cleaned prior to each measurement to prevent additional noise in the acquired data. To clean the optical parts, an air blower for removing dust particles from surfaces, optical grade tissue, and a cleaning spray were used.

In the next chapter, the analysis of the measurements to extract statistical texture features from speckle patterns in line with the image classification outcomes will be discussed.

Chapter 5

Results & Analysis

5.1 Introduction

In this chapter procedures for analyzing the acquired speckle patterns and images from kraft paper samples are described. Classification of different samples of kraft paper with different thermal ageing levels is achieved using a statistical classifier. This classifier uses 24 texture features per image that are generated from the Gray Level Co-occurrence Matrix (GLCM) for each image. For feature reduction and classification, well established algorithms including Principle Component Analysis (PCA), Linear Discriminant Analysis (LDA), and k-Nearest Neighbors (k-NN) were used. Both reflection and transmission mode data were classified to assign the corresponding paper sample to its appropriate class based on its ageing level.

5.2 Data Analysis and Classification System

To design a classification system usually the five following steps are considered[46]: 1) data acquisition and collection, 2) feature extraction or interchangeably feature generation, 3) feature selection (dimension reduction), 4) classifier design, and 5) performance evaluation. The following sections discuss these steps.

5.3 Data Collection

The data set generated using the experimental setups (explained in Chapter 4), has four image classes corresponding to the four ageing levels of the kraft paper samples, *i.e.*, 0, 120, 250, and 400 hours of ageing in the oven at 140ºC. The images classes are equiprobable, *i.e.* all four paper classes have equal data size to prevent biasing the results (50 images per each class of ageing). Images captured by the CCD camera are in 16 bit TIFF format which corresponds to $2^{16} = 65536$ gray levels per image. A summary of properties of the acquired images is listed in Table 5.1.

Table 5.1: Properties of the acquired images

Item	Description
Dimensions (Image size)	1600 (width) × 1200 (Height) pixels
Resolution	300 dpi (both horizontal & vertical)
Laser source	655nm, 5mW Red Laser Diode Module 13×42mm
Bit depth	16 bit
Compression	Uncompressed
Color	Grayscale
Format	TIFF
Average size	2.76 MB

5.4 Feature Extraction

Twenty four texture features were calculated for each image based on Haralick's second-order texture features[1] [11]. Using texture features is straightforward and well established

---

[1] A discussion of reasons for choosing textural features is presented in section 5.4.1.

for classification and machine learning purposes [9]–[11], [40], [41]. Haralick's texture features are bivariate statistics that are computed using pairs of neighboring pixels. To calculate texture features, first of all the Gray Level Co-occurrence Matrix (GLCM)[1] for each image should be provided (see Figure 5.1). We extracted "two" GLCM per each image, corresponding to the two directions of horizontal axis (with $\theta = 0,180°$) and vertical axis (with $\theta = 90,270°$) in the 2-D image coordinates. Afterwards we applied the 12 original Haralick's formulas in each direction which we could get 24 features in total for each image.
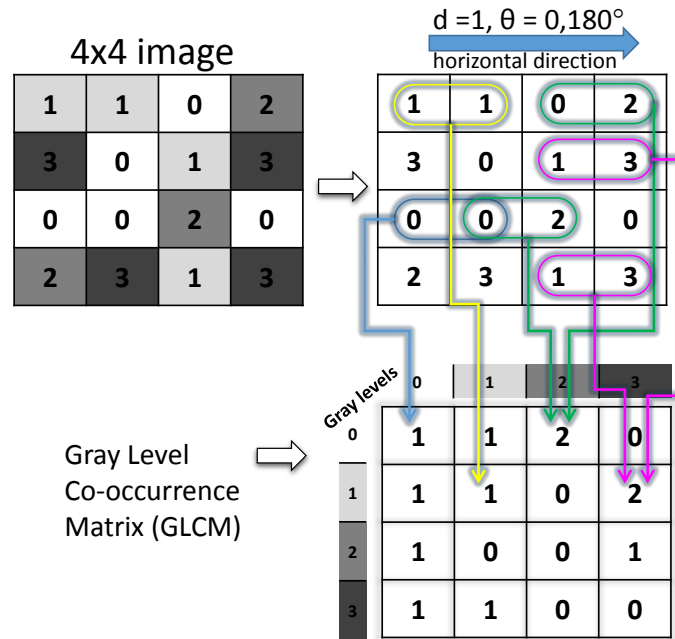
Figure 5.1 Calculation of SGLDM for a sample image with 4 gray levels indicated by 0, 1, 2, and 3 with neighbor index of d=1 in horizontal direction ($\theta = 0,180°$) to extract textural features.

Choosing the number of features to be used depends on the application and experience. To represent as much as possible classification related information from the data, it is common

---

[1] Or equivalently Spatial Gray Level Dependence Matrix (SGLDM).

practice to generate as many features as possible. However proper feature selection methods should be used to prevent feature vectors with large dimensions that could increase computation cost and reduce classification performance. Also it should be noted that the data-set size should be larger than the number of features used[46].

5.4.1 Rationale for Extracting Textural Features from Image Data

There is no solid or unique definition in the literature for texture, however, texture is distinguishable as a visual pattern with some degree of homogeneity or localized statistics. It is a common practice to consider paper's pattern as texture [47]. Texture analysis methods can be categorized as following four groups [48]:

- **Structural (geometrical) methods**: These methods basically define texture by periodic micro-texture elements as primitives and macro-texture patterns as spatial arrangements. In fact a set of primitive building blocks and a repetitive placement rule to construct the texture is required. This approach is mostly suited for synthesis of texture rather than analysis, which is not our goal [48].

- **Statistical methods**: are representing texture by stochastic properties of gray levels of pixels in an image. Second-order statistical methods, which are given based on relation between pair of pixels, have shown better discrimination ability. In this regard, Haralick's textural features calculated based on Gray Level Co-occurrence

Matrix (GLCM) has been known as one of the most popular second-order statistical textural features [11], [49].

- **Model-based methods**: are trying to describe the texture of an image based on the combination of the stochastic models and fractal geometry. These methods have been able to model some natural textures successfully, however complexity in the computation of stochastic model parameters is an issue [48].

- **Transform (signal processing) methods**: represent the texture of the image in a new transformed space according to the texture characteristics such as size or frequency. Gabor, Fourier, and Wavelet transforms have been employed in this field. In [33], Gabor transform method has been used for converting speckle images with the application of fingerprinting paper to detect forgery of signatures. Gabor transform performs based on Gabor filters which has limited practical usefulness in this research since usually there is no single filter resolution to localize spatial structures of the natural textures. Fourier transform has also practical limitations due to the lack of spatial localization. Wavelet transform can represent texture suitably due to variable spatial resolution and freedom in choosing wavelet function from a wide range for a specific application. Wavelet transform is not translation-invariant; this is a drawback of this method [48].

As stated, qualitative visual characteristics of a pattern in texture can be quantified by relating them to the gray levels of its image pixels. In this regard, optical speckle pattern of paper can be considered as texture. Also using texture features is straightforward and well established for classification and machine learning purposes [9]–[11], [40], [41]. In [10] and [41] Haralick textural features have been used for measuring roughness of paper samples for quality assurance application which is better related to the purpose of this research.

In this project Haralick's textural features from statistical approaches were chosen due to their capabilities to identify texture. However, other feature extraction methods can be tested and compared in the future work. A mathematical formula for each feature is provided in [11].

5.5 Feature Selection and Classifier

To handle high dimensional feature space and to overcome the curse of dimensionality, feature selection methods are strongly recommended. Also, of the 24 extracted features for each image, some features could correlated with each other, therefore they may not be highly informative for discrimination purposes. To select the combination of most informative features, various approaches have been proposed. Overall, there is no unique recipe for choosing the method to be used for feature selection [46]. In our work, well-established algorithms, *i.e.* Principle Component Analysis (PCA), Linear Discriminant

Analysis (LDA) and k-Nearest Neighbour (k-NN) methods were used for feature selection and classification.

As a rule of thumb, the number of final selected features, r should be less than one-third of the training data size, D [46]. Let's assume we use 80% of the 50 images of the original dataset for training, $i.e. D = 40$. Therefore, the final number of selected features should satisfy $r \leq 13(\approx \frac{40}{3})$. We used the 10 first features of Principle Component Analysis (PCA).

5.5.1 PCA, LDA, and k-NN

PCA is an unsupervised technique for feature reduction in classification problems. This means that class labels of the data samples are not considered during feature reduction. PCA performs feature selection such that maximum variance of the original data in the feature space is preserved [50].

LDA is a supervised technique which maintains class discrimination by maximizing the "between classes to within class scatterer information", also known as Fisher Discriminant Ratio (FDR), by calculation of covariance matrixes. For example in a 2-class classification problem with 2 features, Fisher Discriminant Ratio (FDR) is defined as

$$FDR = \frac{|\mu_1 - \mu_2|^2}{\sigma_1^2 + \sigma_2^2} \equiv \frac{w^T S_B w}{w^T S_W w} \qquad (5\text{-}1)$$

where μ_1, μ_2 are the mean values and σ_1^2, σ_2^2 are variances of the two classes after projection along the direction of w in (5-1). The direction of w in general is in the m dimensional space which determines best separability of the two classes. S_B is defined as between-classes scatterer matrix and S_W is within-class scatterer matrix. This is equivalent to an eigenvalue problem with corresponding eigen-vectors. In LDA, the goal is to project features such that the maximum difference between the mean classes and minimum variance of classes are maintained simultaneously to maximize the data separation in feature space. In this method, maximum number of features in reduced space is "c - 1" where "c" is number of the classes [50].

Due to popularity and being straightforward, the k-nearest neighbour (k-NN) classifier has been employed in the literature frequently [46], [48], [50], [51]. In this work k-NN classifier is used. K-NN identifies "k" nearest neighbours of an input observation, whose class is unknown, based on a distance measurement criterion. Afterwards, based on the majority of votes for the neighbours' class label, class of the unknown observation will be determined. An example of how k-NN algorithm works is shown in Figure 5.2. A data point ✖ surrounded by 6 neighbors which by the majority of votes is determined as class 4.
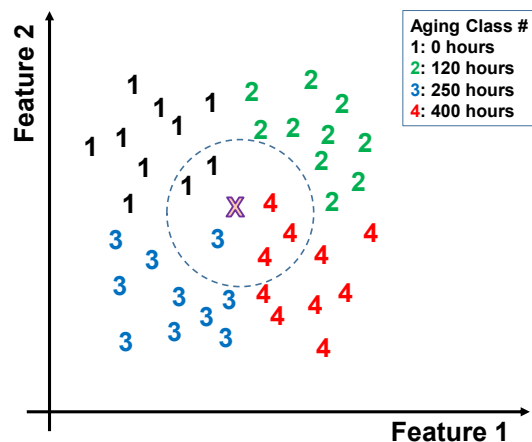
Figure 5.2 Simplified example of a k-NN classifier in a feature space with 2 features and 4 classes.

In general, it is recommended to choose the number of nearest neighbours, *i.e.*, "k" not to be a multiple of the number of the classes to prevent confusion in the voting results[1] [50]. Therefore, as we have 4 classes (corresponding to 4 ageing levels), "k" is chosen to be 3, 5, or 7.

5.6 Performance Evaluation of Classification Results

To evaluate the performance of the classifier used in this work two main approaches have been proposed: cross-validation and confusion matrix [50]. While misclassification error gives an overall estimate of the performance of the classifier, the confusion matrix gives a detailed statistics of the misclassification of each individual class to other classes. Following subsections are a brief description of each approach.

---

[1] For example assume in a 3-class system, we use 6-NN. Consider the special case of 2 votes for class 1, 2 for class 2, and 2 for class 3 from neighbours surrounding a specific data point; there will be no majority vote out of 6. To prevent this situation it is recommended to consider for example a 5-NN classifier since 5 is not a multiple of 3 (i.e. number of classes).

5.6.1 Misclassification Error Percentage Based on Cross-validation

The percentage of misclassified inputs can be used as a measure of error. To estimate the error rate, various cross-validation methods such as "re-substitution", "hold-out", "k-fold", and "leave one out" have been proposed [50]. Among those methods the "leave one out" is commonly used in classification problems with limited date-set sizes. In this cross-validation method, in contrast to re-substitution method, independence of the training and test data-sets is maintained. In the Leave-One-Out Cross-Validation (LOOCV) method, one observation from the original data-set is excluded and the resulting misclassification error is obtained. This procedure is repeated until each observation data point is excluded from training set and treated as a testing point. The final misclassification error is calculated as the average of all misclassification errors [46], [50].

5.7 PCA reduction, k-NN classification

After computing principle components based on texture features of 40 images in each of the four ageing classes, the following results for principle components in each imaging mode are calculated and listed in Table 5.2. Each principle component is a combination of the 24 original features and the "Explained" column indicates the percentage of the total variance explained by each principle component.

Table 5.2 Principle Components, sorted

Rank	Percentage of data explained by "x"th Principle Component			
	Reflection Explained%	Total cumulative coverage%	Transmission Explained%	Total cumulative coverage %
1st	61.7112	61.7112	63.5952	63.5952
2nd	16.3330	78.0442	23.3346	86.9298
3rd	11.6106	89.6548	6.3757	93.3056
4th	4.8106	94.4655	2.7377	96.0433
5th	2.5924	97.0578	1.8152	97.8585
6th	1.8114	98.8693	0.9956	98.8542
7th	0.5171	99.3863	0.6340	99.4882
8th	0.2482	99.6345	0.2404	99.7286
9th	0.1164	99.7509	0.0963	99.8248
10th	0.0968	99.8476	0.0602	99.8850

This simply means that the 1st principle component of feature space of the reflection mode[1] data, covers only 61.71% of all the information included in all classes, while the 10th principle component covers 0.0968% of the data. We chose the first 10 principle components as the dimension of the new reduced space which covers 99.84% of data in reflection mode and 99.88% of transmission mode data. To better understand the acquired data-points, let's consider Figure 5.3 which shows the projection of all the classes in the principal component space which has been represented by the first three highest rank eigenvectors for reflection and transmission mode. As a qualitative inspection, there is no visual separation of data in the projected space.

---

[1] Reflection mode considers the sample as a reflective object, in contrast to transmission mode which laser illumination passes through the sample, as stated in subsection 4.4.2.

(a)   (b)
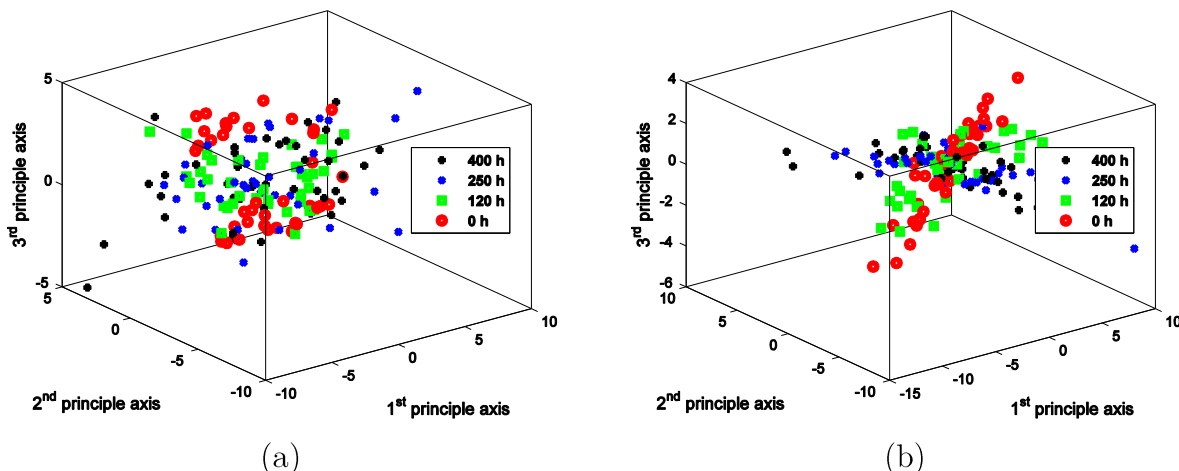
Figure 5.3 Representation of the data features projected to first three principal components by PCA method in (a) reflection and (b) transmission mode. Each point corresponds to an observation of a paper sample. Different classes of ageing of paper for each data-point have been identified by red○, green□, blue×, and black + respectively for 0, 120, 250, and 400 hours of thermal ageing.

In the next step a k-NN classification was used based on the PCA data with the 10 first features. Table 5.3 shows a comparison between misclassification error rates for each data acquisition mode. This analysis is based on a Leave One Out Cross Validation (LOOCV) estimate on the 80% of the original dataset as training set[1].

Table 5.3 Percentage of misclassification based on LOOCV and 10-fold cross validation error estimate method for k-NN classifier applied on reduced space of feature space with 10 first principle components of PCA.

k-NN classifier	Misclassification %			
k	Reflection Mode		Transmission Mode	
	LOOCV	10-fold	LOOCV	10-fold
3-NN	19.38	26.25	40.63	53.75
5-NN	25.63	35.00	46.88	54.38
7-NN	25.63	29.38	48.13	60.00

---

[1] We kept 20% of the data as unseen data to test the classifier. This approach gives a more realistic estimate of the misclassification error rate and prevents biasing of the classifier.

5.8 LDA reduction, k-NN classification

As we have 4 classes of data, exactly $3 = (4 - 1)$ linear discriminant components yield for the data-set. Figure 5.4 shows LDA projection in the new reduced space of feature vectors for both reflection and transmission mode speckle patterns data.

(a)   (b)

Figure 5.4 Representation of the data projected to LDA space in (a) reflection and (b) transmission mode. Each point corresponds an observation on a paper sample. Different classes of ageing of paper for each data-point have been identified by red, green, blue, and black ○ respectively for 0, 120, 250, and 400 hours of thermal ageing Discrimination of 4 classes is visible.

The k-NN classification for the 3 LDA projected features has been performed for $k = 3, 5, 7$.

Table 5.4 shows a comparison of the misclassification error rates for each data acquisition mode based on Leave One Out Cross Validation estimate in this step.

Table 5.4 Misclassification % based on Leave One Out Cross Validation (LOOCV) and 10-fold cross validation error estimate method for k-NN classifier applied on reduced space of feature space with 3 LDA based features.

k-NN classifier	Misclassification %			
k	Reflection Mode		Transmission Mode	
	LOOCV	10-fold	LOOCV	10-fold
3-NN	1.88	1.88	3.75	5.63
5-NN	1.25	1.25	5	5.63
7-NN	1.25	1.25	5.63	4.38

5.9 LDA reduction, Linear Discriminant classification

This approach is based on the LDA projection where the classifier is a linear function of the feature vectors. The resulting misclassification rate for linear discriminant classifier on LDA projected features is 1.25% in reflection mode and 3.75% in transmission mode. In the last step of analysis, for each class, 10 data points were provided to the classifier. Due to good discrimination of the classes, test data projected to the same region of the corresponding class. This is specially promising for reflection mode data in comparison with the transmission mode data. Following figures shows the representation of data-points corresponding to each ageing level of paper samples in LDA space.
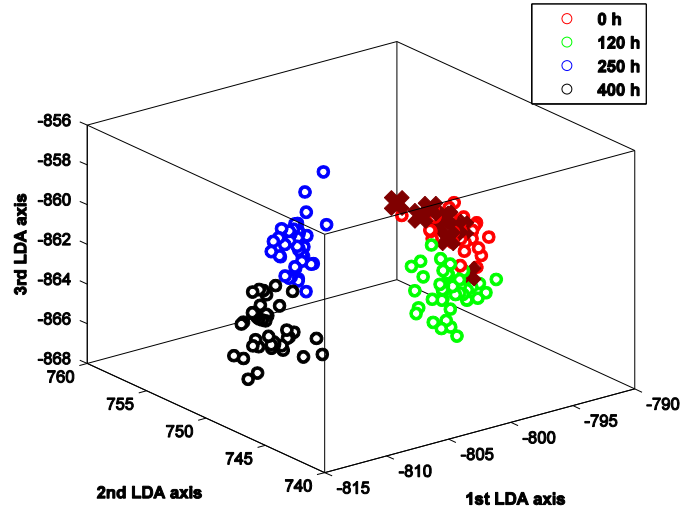
Figure 5.5 Representation of the data projected to LDA space for reflection mode speckle data. Red "×"s corresponds to the test data of new paper sample which is provided to the classifier for the first time. It is evident that they are projected to the correct region of feature space which has been verified by misclassification error rate of 2.5%.
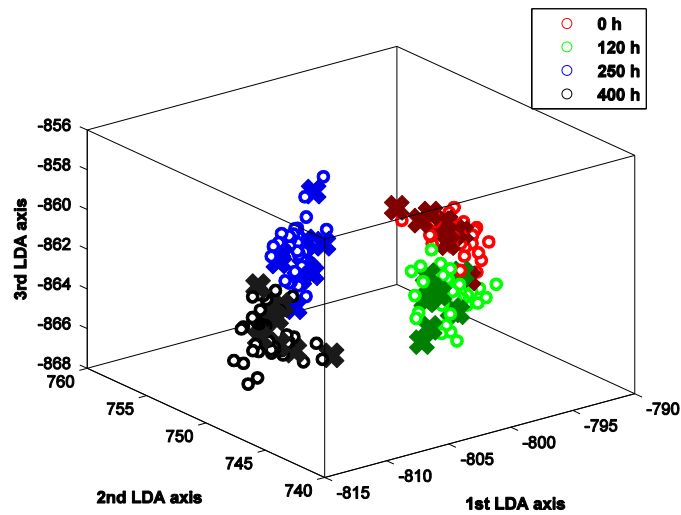
Figure 5.6 Representation of all four classes of reflected mode speckle data in LDA space. Bold "×"s correspond to the test data of each class which is provided to the classifier for the first time.

63

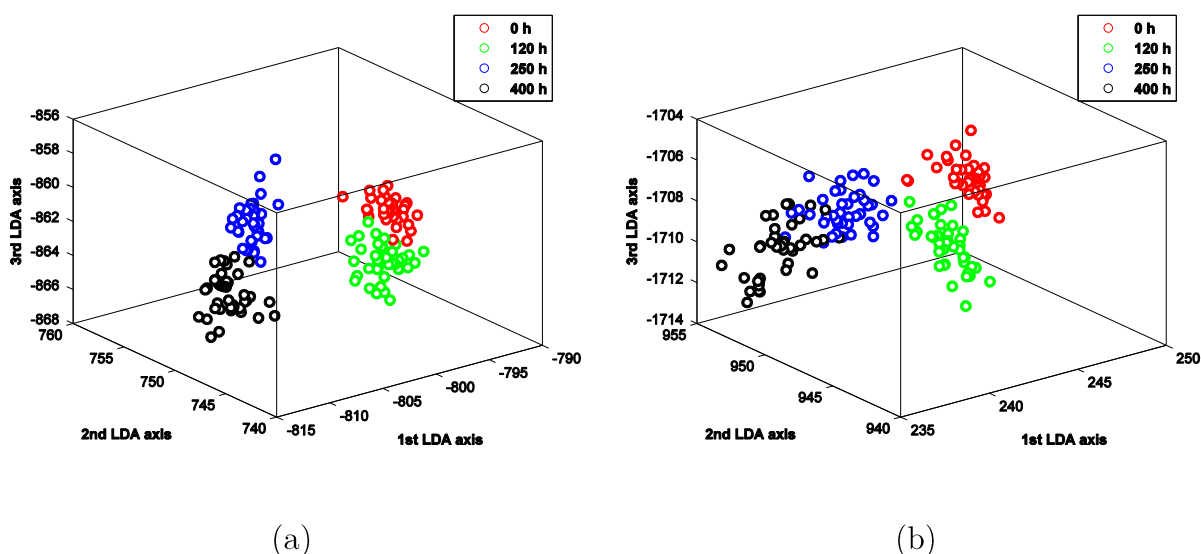(a)   (b)
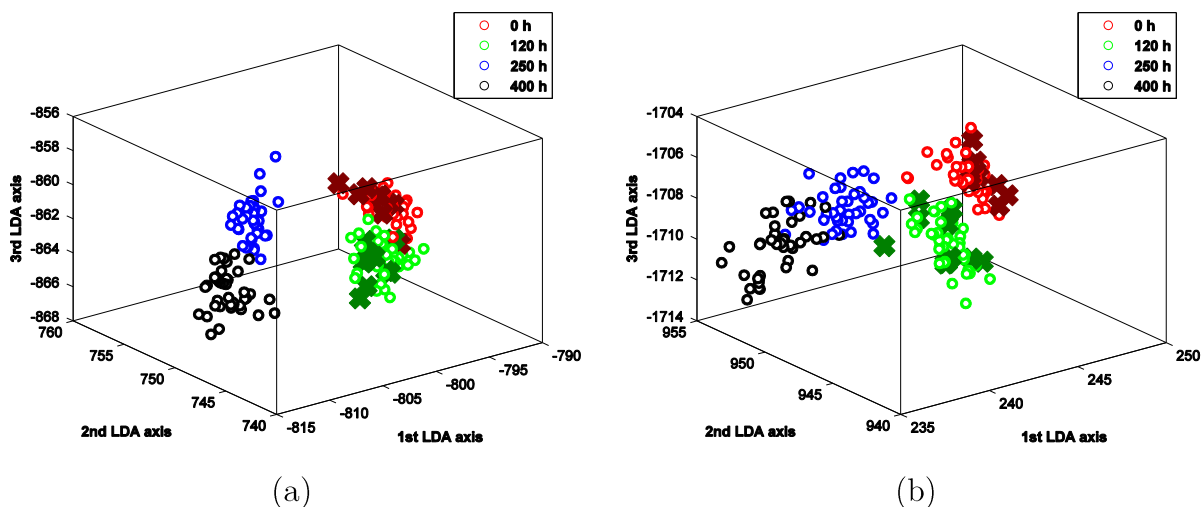
Figure 5.7 Representation of the data projected to LDA space in (a) reflection and (b) transmission mode. Each point corresponds to an observation on a paper sample. Different classes of ageing of paper for each data-point have been identified by red, green, blue, and black ○ respectively for 0, 120, 250, and 400 hours of thermal ageing Discrimination of 4 classes is visible.

5.10 Confusion Matrix and Its Interpretation

For a classification problem with l classes, confusion matrix is a $l \times l$ matrix whose $(ij)^{\text{th}}$ element shows how many data points with true class label of "i" have been mistakenly classified to the class "j". In fact, confusion matrix is another performance evaluation measure for a classifier, indicating classes with higher probability of misclassification or interchangeably determines the classes in which originate higher confusion [50]. Figure 5.8 shows a detailed interpretation of the elements of confusion matrix computed for 40 test data points (= 10 data points per class $\times$ 4 thermal ageing classes).
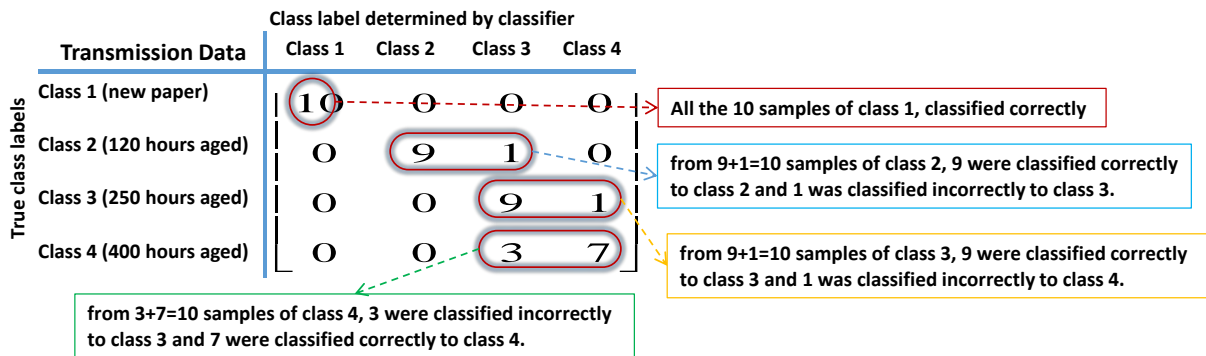
Figure 5.8 Interpretation of confusion matrix for case of 10 datapoints per class in transmission mode.

It is desired to have non-zero diagonal elements and zero non-diagonal elements which corresponds to 100% classification accuracy. The confusion matrix for the two mode of reflection and transmission data with k-NN classifier is presented in Table 5.5.

Table 5.5. Comparison of confusion matrix for k-NN classifier in two modes.

Confusion Matrix	
Transmission	Reflection
C_{trans}	C_{ref}

$$\begin{vmatrix} 10 & 0 & 0 & 0 \\ 0 & 9 & 1 & 0 \\ 0 & 0 & 9 & 1 \\ 0 & 0 & 3 & 7 \end{vmatrix} \quad \begin{vmatrix} 10 & 0 & 0 & 0 \\ 0 & 10 & 0 & 0 \\ 0 & 0 & 9 & 1 \\ 0 & 0 & 0 & 10 \end{vmatrix}$$

It is apparent that C_{ref} has less non-zero off-diagonal elements which is an indicator of less misclassification error for reflection mode in comparison with C_{trans} for transmission mode. This is also complying with the previous error estimates confirming better classification performance for reflection mode data. We should point out that according to the confusion matrix, most of the confusion has been occurred for class 4 and 3 in transmission mode.

Also class 1 has been correctly classified to its real class label, however for a better statistical conclusion based on confusion matrix for ageing phenomenon in real paper samples of the transformers, it is recommended to increase number of ageing classes and number of data points in each class.

5.11 Summary of classification results

In Table 5.6 a summary of classification performance evaluation is listed.

Table 5.6 Comparison between misclassification errors for different classification scenarios

		Misclassification Error %	
		Reflection Mode	**Transmission Mode**
LOOCV estimate	3-NN	1.88	3.75
	5-NN	1.25	5
	7-NN	1.25	5.63
Unseen Test	3-NN	2.5	13.9
	5-NN	0	13.9
	7-NN	0	11.6
	LDA	1.25	3.75
	LDA (unseen)	2.5	11.6

Following is a summary of the classification performance of the methods used in this thesis.

- Misclassification error estimate:
    - In k-NN classifier by increasing the "k" (neighbor of each unknown data-point to be classified), misclassification error estimate based on LOOCV[1] decreases from 1.88% for k=3 to 1.25% for k=5.

---

[1] LOOCV: Leave One Out Cross Validation

- o In k-NN classifier for transmission mode data, by increasing "k", misclassification error estimate based on LOOCV increases from 3.75% for k=3 to 5.63% for k=7.

- o In LDA based classification, speckle data acquired from reflection mode, was classified more accurately than transmission mode data.

- o The error estimate shows better classification rate for reflection mode data rather than transmission mode data.

- Real classification error for unseen data-points;
  - o 3-NN classifier shows higher misclassification error than 7-NN classifier.

  - o 5-NN and 7-NN classified all 40 unseen images (10 image per each class) correctly to their real classes which results in zero misclassification error for reflection mode data. This is a very satisfactory result however for a more generalized statistical conclusion, it should be tested on more unseen inputs.

  - o LDA based classification for unseen data has higher error rate for transmission mode than reflection mode.

  - o Linear classification based on LDA reduced features shows better performance in comparison to k-NN classifier for transmission mode data. However, for reflection mode data it is vice versa, *i.e.* k-NN shows less error for reflection mode data.

o   Misclassification error for transmission mode is higher than reflection mode which complies with error estimates of LOOCV for both k-NN and linear classifier based on LDA feature reduction.

Highest average misclassification error resulted for k-NN classification on transmission mode data. Lowest average misclassification error resulted for k-NN classification on reflection mode data. In general, results show misclassification error for the k-NN classifier is lower for reflection mode data in comparison to transmission mode data.

Chapter 6

Conclusions and Future Work

6.1 Discussions

In this thesis, it has been shown that using optical speckle phenomenon is a practical approach for the classification of kraft paper with different thermal ageing levels. Speckle patterns due to interaction of laser illumination with the structure of the kraft paper, were captured with a CCD camera in both transmission and reflection mode. The acquired images were processed for texture feature extraction and classification.

Our work shows that well-known classification methods such as "k Nearest Neighbors (k-NN)" could give very good classification results. This conclusion is confirmed by misclassification error rate of maximum 2.5% in the classification of 4 ageing level of the paper samples with the optical speckle setup in the reflection mode. Also, the confusion matrix shows there is less confusion for detecting new kraft paper samples but as the ageing level increases, there is more confusion in detecting paper samples. For the case of transmission mode speckles patterns, the obtained results show that 30% of samples with

400 hours of ageing were misclassified to class 3 (with 250 hours of ageing). In reflection mode, less confusion among classes was detected, *i.e.* 10 % of class 3 samples were misclassified to class 4 (see Table 5.5). Two points should be noted: 1) for better evaluation of our methodology to acquire data and classification, more data samples with increased ageing levels should be tested, and 2) in general reflection mode data were better classified into corresponding classes in comparison to the transmission mode data. This was verified by both cross validation and confusion matrix methods in the classification phase which can be related to the nature of the optical phenomenon involved in reflection and transmission. As a qualitative explanation, in the reflection mode, with neglecting the absorption of incident light to the paper material, interaction of light and matter occurs just in the 2-dimensional surface of the paper with its micrometer range random fiber structure. Therefore, the reflected optical wave is mainly altered due to randomness of paper surface. On the other hand, in the transmission mode, the laser beam passes through volume of oil-impregnated paper which could be several optical wavelength in depth and multiple scattering occurs. The passing beam not only contains surface information but also included alterations due to internal random structure of the paper in volume. On the other hand, good classification results for the reflection mode is promising. Regarding future implementation of the system, implementation of the reflection mode setup could be more practical and non-invasive. For transmission mode setup, a paper sample should be removed

from the insulation whereas in the reflection mode, the illuminator and the detector can be

placed close to the surface of paper without the requirement of removing a sample of paper.

6.2 Future Work Recommendations

Sensor based implementation with fiber-optics for on-line monitoring: Optical

speckle based method to classify ageing levels of kraft paper can be implemented in on-line

condition monitoring equipment for power transformers. Developing a sensor based speckle

setup has the benefit of integration with the already installed monitoring hardware.

Potential of using fiber-optics for this specific application should be investigated in the

future researches.

Ageing classification for other cellulose-based insulation materials: Another

possibility of using our optical speckle method is to investigate other cellulose-based

insulation materials, such as pressboards in power transformers.

Accelerated electrical ageing: In this project, accelerated thermal aging has been used

to investigate the effect of ageing due to thermal heating on kraft paper. The reason was

that it has been assumed that the thermal stress is the main contributing factor leading to

insulation degradation. For better evaluation of the condition of kraft paper as transformer

insulation, it would be beneficial to mimic the real operating condition of the transformer

in presence of electric field and voltage stress. This will require preparation of proper test setup with the ability to apply and control both the thermal and electrical stresses.

Recommendation for methodology: The effect of variation in laser wavelength and deflection angle toward the sample on the speckle patterns from the paper samples can be investigated to find the optimum condition with lowest misclassification errors.

Recommendation for classification: Other classification methods can be implemented to address comparison of different classifying approaches. This project investigated a feasibility study in which ageing phenomenon was modeled by accelerated thermal ageing. For a real implementation, it is advisable to take real aged paper samples from de-tanked transformers to build a more realistic ageing database for classification purposes.

References

[1]   J. H. Harlow, Ed., *Electric Power Transformer Engineering, Third Edition, Volume 2*. CRC Press, 2012, p. 693.

[2]   "Electricity Exports," 2014. [Online]. Available: https://www.hydro.mb.ca/corporate/electricity_exports.shtml. [Accessed: 04-Aug-2014].

[3]   D. Klemm, B. Heublein, H.-P. Fink, and A. Bohn, "Cellulose: Fascinating Biopolymer and Sustainable Raw Material," *ChemInform*, vol. 36, no. 36, Sep. 2005.

[4]   P. Verma, "Condition monitoring of transformer oil and paper," Ph.D. thesis, Thapar Institue of Engineering & Technology, 2005.

[5]   Erkki Alarousu, "Low coherence interferometry and optical coherence tomography in paper measurements," Ph.D. thesis, University Of Oulu, Fineland, 2006.

[6]   R. J. Liao, C. Tang, L. J. Yang, and S. Grzybowski, "Thermal aging micro-scale analysis of power transformer pressboard," *IEEE Trans. Dielectr. Electr. Insul.*, vol. 15, no. 5, pp. 1281–1287, 2008.

[7]   A. Teleman, C. Östlund, J. Nordström, P.-Å. Johansson, and H. Vomhoff, "Analysis of paper surface topography under compression," 2004. [Online]. Available: www.innventia.com/STFI-Packforsk report cw217.pdf.

[8]   Manitoba Hydro, "The Manitoba Hydro-Electric Board 62nd Annual Report, 2012-2013," 2013.

[9]   P. Jacquot and J.-M. Fournier, Ed., "Interferometry in Speckle Light, Theory and Applications," in *Proceedings of the International Conference 25-28 September 2000, Lausanne, Switzerland*, 2000.

[10]   A. Pino and J. Pladellorens, "Measure of roughness of paper using speckle," *Proc. SPIE*, vol. 7432, no. 1, pp. 74320E–1–74320E–9, Aug. 2009.

[11] R. M. Haralick, K. Shanmugam, and I. Dinstein, "Textural Features for Image Classification," *IEEE Trans. Syst. Man. Cybern.*, vol. 3, no. 6, 1973.

[12] M. Francon, *Laser Speckle and Applications in Optics*, Translated. ACADEMIC PRESS INC., 1979.

[13] "IEEE Std C57.12.80-2010, IEEE Standard Terminology for Power and Distribution Transformers." 2010.

[14] M. J. Heathcote, "Electric Power Transformer Engineering, Third Edition [Book Reviews]," *IEEE Power Energy Mag.*, vol. 11, no. 5, pp. 94–95, Sep. 2013.

[15] H. Holik, Ed., *Handbook of Paper and Board (Google eBook)*. John Wiley & Sons, 2013, p. 800.

[16] "IEEE.C57.100-2011, IEEE Standard Test Procedure for Thermal Evaluation of Insulation Systems for Liquid-Immersed Distribution and Power Transformers." Standard, IEEE Power Energy Society, 2012.

[17] W. T. Shugg, *Handbook of Electrical and Electronic Insulating Materials*. Van Nostrand Reinhold, 1986, p. 598.

[18] T. A. Prevost and T. V. Oommen, "Cellulose insulation in oil-filled power transformers: Part I - History and development," *IEEE Electr. Insul. Mag.*, vol. 22, pp. 28–34, 2006.

[19] P. J. Baird, H. Herman, G. C. Stevens, and P. N. Jarman, "Non-destructive measurement of the degradation of transformer insulating paper," *IEEE Trans. Dielectr. Electr. Insul.*, vol. 13, no. 1, pp. 309–318, 2006.

[20] T. K. Saha, "Review of Modern Diagnostic Techniques for Assessing Insulation Condition in Aged Transformers," in *IEEE Transactions on Dielectrics and Electrical Insulation*, 2003, vol. 10, pp. 903–917.

[21] T. K. Saha and P. Purkait, "Understanding the impacts of moisture and thermal ageing on transformer's insulation by dielectric response and molecular weight measurements," *IEEE Trans. Dielectr. Electr. Insul.*, vol. 15, pp. 568–582, 2008.

[22] R. J. Liao, B. Xiang, L. J. Yang, C. Tang, and H. G. Sun, "Study on the thermal aging characteristics and bond breaking process of oil-paper insulation in power

transformer," in *Conference Record of IEEE International Symposium on Electrical Insulation*, 2008, pp. 291–296.

[23] R. Liao, C. Tang, L. Yang, and H. Chen, "Thermal aging studies on cellulose insulation paper of power transformer using AFM," in *Proceedings of the IEEE International Conference on Properties and Applications of Dielectric Materials*, 2007, pp. 722–725.

[24] "IEEE C57.125-1991, IEEE Guide for Failure Investigation, Documentation, and Analysis for Power Transformers and Shunt Reactors." 1991.

[25] "IEEE Std C57.140-2006, IEEE Guide for the Evaluation and Reconditioning of Liquid Immersed Power Transformers." 2006.

[26] V. Der S.M. Gubanski (chair), P. Boss, G. Csépes, V. Houhanessian, J. Filippini, P. Guuinic, U. Gäfvert, and W. Z. Karius, J. Lapworth, G. Urbani, P. Werelius, "Dielectric response methods for diagnostics of power transformers," *IEEE Electr. Insul. Mag.*, vol. 19, no. 3, pp. 12–18, May 2003.

[27] "Transformer Condition Monitoring Practices with A Special Approach for Detection of Electric Arcs," 2006. [Online]. Available: http://www.energymanagertraining.com/Journal/19102006/TransformerCondition MonitoringPracticesWithASpecialApproachforDetectionofElectricArcs.pdf.

[28] D. H. Shroff and A. W. Stannett, "A review of paper aging in power transformers," *IEE Proceedings C Generation, Transmission and Distribution*, vol. 132. p. 312, 1985.

[29] R. J. Heywood, A. M. Emsley, and M. Ali, "Degradation of cellulosic insulation in power transformers. Part 1: Factors affecting the measurement of the average viscometric degree of polymerisation of new and aged electrical papers," *IEE Proceedings - Science, Measurement and Technology*, vol. 147. p. 86, 2000.

[30] J. C. Dainty, *Laser Speckle and Related Phenomena*. Springer-Verlag Berlin Heidelberg New York, 1975.

[31] G. H. Kaufmann, *Advances in Speckle Metrology and Related Techniques*. WILEY-VCH Verlag & Co. KGaA, Boschstr. 12, 69469 Weinheim, Germany, 2011.

[32]   W. An, "Industrial Applications of Speckle Techniques, Measurement of Deformation & Shape," Ph.D thesis, KTH (Royal Institute of Technology), Stockholm, Sweden, 2002.

[33]   B. E. A. Saleh, M. C. Teich, S. Editor, and J. W. Goodman, *Fundamentals of Photonics (Wiley Series in Pure and Applied Optics)*. 1991, p. 992.

[34]   P. Hariharan, *Basics of interferometry*. Boston : Academic Press, 1992, p. 213.

[35]   J. W. Goodman, *Speckle phenomena in optics: theory and applications*. Roberts & Company, 2007, p. 387.

[36]   "Aperture." [Online]. Available: http://en.wikipedia.org/wiki/Aperture. [Accessed: 07-Oct-2014].

[37]   J. I. Trisnadi, "Speckle contrast reduction in laser projection displays," *Proc. Soc. PHOTO-OPTICAL Instrum. Eng.*, vol. 4657, pp. 131–137, 2002.

[38]   A. Lifjeld, "Reduction of speckle contrast in laser based HDTV projection displays," M.Sc. thesis, Norwegian University of Science and Technology (NTNU), 2007.

[39]   D. Brogioli, "Near Field Speckles," Ph.D thesis, Cornell University, 2009.

[40]   A. Sharma, L. Subramanian, and E. A. Brewer, "Paper Speckle: microscopic fingerprinting of paper," in *Proceedings of the 18th ACM conference on Computer and communications security - CCS '11*, 2011, p. 99.

[41]   A. Pino, "Roughness measurement of paper using speckle," *Opt. Eng.*, vol. 50, no. 9, p. 093605, Sep. 2011.

[42]   M. Nicklawy and A. Hassan, "Characterizing surface roughness by speckle pattern analysis," *J. Sci. Ind. Res.*, vol. 68, no. 2, pp. 118–121, 2009.

[43]   "ASTM D5642 - 09, Standard Test Method for Sealed Tube Chemical Compatibility Test." 2009.

[44]   P. Verma, D. S. Chauhan, and P. Singh, "Effects on tensile strength of transformer insulation paper under accelerated thermal and electrical stress," in *Annual Report - Conference on Electrical Insulation and Dielectric Phenomena, CEIDP*, 2007, pp. 619–622.

[45] "analySIS® 3.0 The EFI Module." [Online]. Available: ftp://ftp.ccmr.cornell.edu/utility/FEI temp/AnalySIS docs/add-ins/EFI.PDF.

[46] S. Theodoridis and K. Koutroumbas, *An introduction to Pattern Recognition: A Matlab Approach*, USA. Academic Press (Elsevier), 2010, p. 216.

[47] T. A. Pham, "Optimization of Texture Feature Extraction Algorithm, M.Sc. thesis in computer engineering," Delft University of Technology, Netherlands, 2010.

[48] M. S. Andrzej Materka, "Texture analysis methods - a review," COST B11 report, Technical University of Lodz, Institute of Electronics, Brussels, 1998.

[49] Robert M.Haralick Linda G. Shapiro, *Computer and Robot Vision*, vol. 1. Addison-Wesley publishing company, 1992.

[50] S. Theodoridis and K. Koutroumbas, *Pattern Recognition, Fourth Edition*. Academic Press (Elsevier), 2009, p. 961.

[51] I. Kitanovski, B. Jankulovski, I. Dimitrovski, and S. Loskovska, "Comparison of feature extraction algorithms for mammography images," in *2011 4th International Congress on Image and Signal Processing*, 2011, vol. 2, pp. 888–892.

[52] "Envirotemp FR3 Fluid in Cold Climate Applications." [Online]. Available: http://www.spxtransformersolutions.com/assets/documents/FR3ColdTempFAQNo v08.pdf. [Accessed: 04-Sep-2014].

[53] "ENVIROTEMP ® FR3™ FLUID Brouchure." [Online]. Available: http://www.nttworldwide.com/docs/fr3brochure.pdf. [Accessed: 04-Sep-2014].

[54] "Paper Strength properties." [Online]. Available: http://www.europapier.com/service/knowhow/testingpaper/strength-properties. [Accessed: 06-Oct-2014].

[55] "Luminol electrical insulating oil by PetroCanada Technical Data." [Online]. Available: http://lubricants.petro-canada.ca/resource/download.aspx?type=TechData&iproduct=1780&language=en. [Accessed: 04-Sep-2014].

[56] "VOLTESSO™   transformer   oil."   [Online].   Available: http://www.mobil.com/Canada-English/Lubes/PDS/IOCAENINDMOVOLTESSO.aspx. [Accessed: 04-Sep-2014].

Appendix A – Textural features

The following textural features have been used based on the formulas provided in [11].

Feature	Description	Formula
F1	Angular second moment (ASM) Energy Measure of uniformity of an image; similar pixels results in large ASM.	$\sum_{i=1}^{N}\sum_{j=1}^{N} p_{(d,\theta)}(i,j)^2$
F2	Contrast Measure of intensity or gray-level variations between the reference pixel and its neighbor.	$\sum_{\substack{n=1, \\ n=\|i-j\|}}^{N} n^2 \left\{ \sum_{i=1}^{N}\sum_{j=1}^{N} p_{(d,\theta)}(i,j) \right\}$
F3	Correlation Measure of linear dependency of gray level values in the co-occurrence matrix; for uncorrelated=0, perfectly correlated=1.	$(\sigma_x \sigma_y)^{-1}\left(\left(\sum_{i=1}^{N}\sum_{j=1}^{N} p_{(d,\theta)}(i,j) \right) - \mu_x \mu_y \right),$ $\mu_x = \sum_{i=1}^{N}\sum_{j=1}^{N} i.p_{(d,\theta)}(i,j),$ $\mu_y = \sum_{i=1}^{N}\sum_{j=1}^{N} j.p_{(d,\theta)}(i,j)$ $\sigma_x = \left(\sum_{i=1}^{N}\sum_{j=1}^{N} (i-\mu)^2.p_{(d,\theta)}(i,j) \right)^{\frac{1}{2}},$ $\sigma_y = \left(\sum_{i=1}^{N}\sum_{j=1}^{N} (j-\mu)^2.p_{(d,\theta)}(i,j) \right)^{\frac{1}{2}}$
F4	Variance (Sum of Squares)	$\sum_{i=1}^{N}\sum_{j=1}^{N} (i-\mu)^2 p_{(d,\theta)}(i,j)$

	Measure of the dispersion of the values around the mean of combinations of reference and neighbor pixels.	
F5	Inverse Difference Moment (IDM) Measure of the local homogeneity of an image	$\displaystyle\sum_{i=1}^{N}\sum_{j=1}^{N}\frac{1}{1+(i-j)^2}p_{(d,\theta)}(i,j)$
F6	Sum Average	$\displaystyle\sum_{i=2}^{2N}i.\,p_{x+y}(i)$ $\displaystyle p_{(x+y)}(k)=\sum_{i=1}^{N}\sum_{j=1}^{N}p_{(d,\theta)}(i,j),\,k=i+j$
F7	Sum Variance	$\displaystyle\sum_{i=2}^{2N}(i-F_6)^2.\,p_{x+y}(i)$
F8	Sum Entropy	$\displaystyle-\sum_{i=2}^{2N}p_{x+y}(i)\log(p_{x+y}(i))$
F9	Entropy Measure of the amount of chaos or disorder.	$\displaystyle-\sum_{i=1}^{N}\sum_{j=1}^{N}p_{(d,\theta)}(i,j)\log(p_{(d,\theta)}(i,j))$
F10	Difference Variance	$\displaystyle\sum_{i=1}^{N}(i-F'_{10})^2.\,p_{x-y}(i)$ $\displaystyle p_{x-y}(k)=\sum_{i=1}^{N}\sum_{j=1}^{N}p_{(d,\theta)}(i,j),\,k=|i-j|$ $\displaystyle F'_{10}=\sum_{i=1}^{N}i.\,p_{x-y}(i)$

F11	Difference Entropy	$-\sum\limits_{i=1}^{N} p_{x-y}(i)\log(p_{x-y}(i))$
F12	Information Measures of Correlation Feature 1, 2	$F_{12} = \dfrac{HXY - HXY1}{\max(HX, HY)}$, $F_{13} = (1 - \exp[-2(HXY2 - HXY)]^{\frac{1}{2}})$ $p_x(i) = \sum\limits_{j=1}^{N} p_{(d,\theta)}(i,j)\,, p_y(j) = \sum\limits_{i=1}^{N} p_{(d,\theta)}(i,j)$ $HX = -\sum\limits_{i=1}^{N} p_x(i)\log(p_x(i))$ $HY = -\sum\limits_{i=1}^{N} p_y(i)\log(p_y(i))$ $HXY = -\sum\limits_{i=1}^{N}\sum\limits_{j=1}^{N} p_{(d,\theta)}(i,j)\log(p_{(d,\theta)}(i,j))$ $HXY1 = -\sum\limits_{i=1}^{N}\sum\limits_{j=1}^{N} p_{(d,\theta)}(i,j)\log(p_x(i)p_y(j))$ $HXY2 = -\sum\limits_{i=1}^{N}\sum\limits_{j=1}^{N} p_x(i)p_y(j)\log(p_x(i)p_y(j))$

Appendix B - Optical Setup Part Details

The following part list have been used to implement the optical speckle setups discussed in

chapter 4:

Part	Picture	Part	Picture
423 (High performance low-profile ball bearing linear translation stage) from kit MK-6		LH-2 (Fixed Lens Mount) from kit MK-4	
360-45 (Angle Bracket) from kit MK-6		LH-OBJ (Microscope Objective Mount) From ki MK-4	
481-A (Rotation Stage 360 coarse, 5° fine rotation, micrometer) from kit MK-6		B-2SA (Stainless steel slotted base) from kit MK-3	
V100 (Mirror mount) from kit MK-6		PS-2 (Precision Ground Stainless Steel Optical Pedestal) from kit MK-3	

PS-0.125 (Optical Pedestal Spacer) from kit MK-3		PS-F (Pedestal Base Clamping Fork) from kit MK-3	
SP-2, SP-3 (Precision Ground Stainless Steel Optical Mounting Post) from kit MK-3		VPH-2, VPH-3 (Standard Optical Post Holder) from kit MK-3	
M-P100-P (Platform optical mount 1 in) from kit MK2		SP-6 , SP-8 (Precision Ground Stainless Steel Optical Mounting Post) from kit MK2	
CA-1 (Right-angle post clamp) from kit MK2		AC-1A (Universal Fixed Lens Mount) from kit MK2	
SK-25A, M-SK-M6A (1/4-20 Black Oxide Screw Kit)		M-SK-M6A	